AD-A108 071 GRUMMAN AEROSPACE CORP BETHPAGE NY RESEARCH DEPT F/G 20/4
NONLINEAR ANALYSIS OF INTERFERING BODIES IN SUPERSONIC FLOW.(U)
JUL 81 F MARCONI F49620-80-C-0044
UNCLASSIFIED RE-631 AFOSR-TR-81-0771 NL

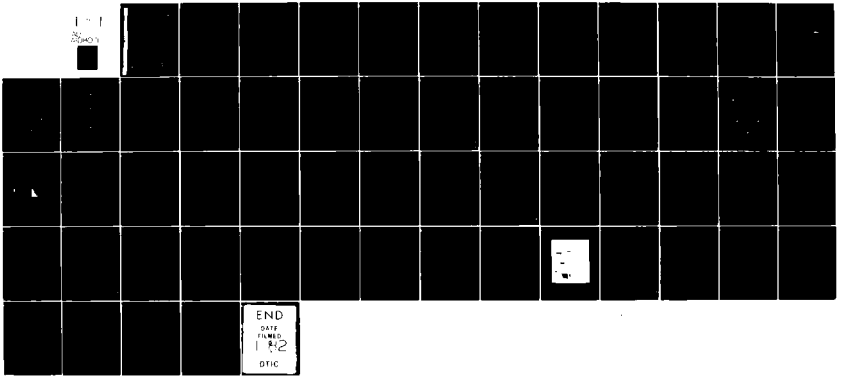

END
DATE FILMED
12
DTIC

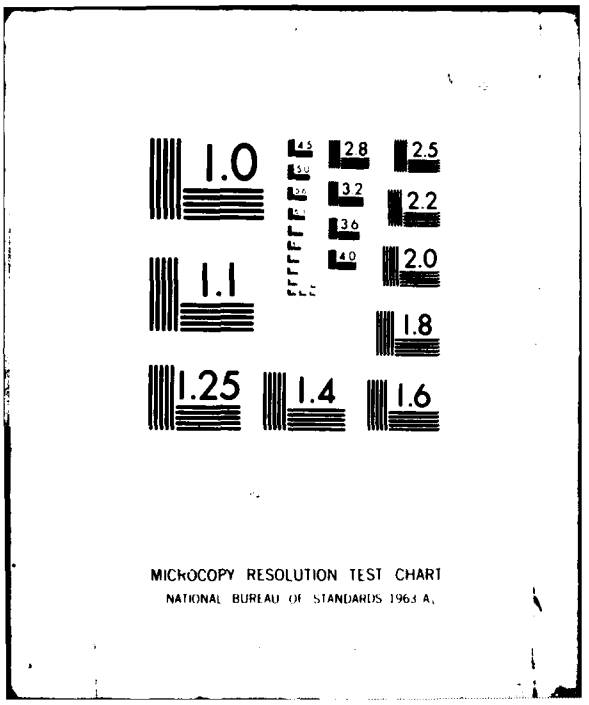
1.0
1.1
1.25
1.4
1.6
1.8
2.0
2.2
2.5
2.8
3.2
3.6
4.0
MICROCOPY RESOLUTION TEST CHART
NATIONAL BUREAU OF STANDARDS 1963 A

LEVEL II

12

AFOSR-TR

RE-631

NONLINEAR ANALYSIS OF INTERFERING BODIES IN SUPERSONIC FLOW

Frank Marconi

Grumman Aerospace Corporation
Bethpage, New York 11714

Under Contract No. F49620-80-C-0044

Final Report
for Period 17 March 1980 - 16 May 1981

July 1981

Prepared for
AIR FORCE OFFICE OF SCIENTIFIC RESEARCH
Bolling Air Force Base
Washington, D.C. 20332

UNCLASSIFIED

SECURITY CLASSIFICATION OF THIS PAGE (When Data Entered)

REPORT DOCUMENTATION PAGE

READ INSTRUCTIONS BEFORE COMPLETING FORM

1. REPORT NUMBER: AFOSR-TR- 81 -0771	2. GOVT ACCESSION NO.: AD-A108 071
3. RECIPIENT'S CATALOG NUMBER	
4. TITLE (and Subtitle): NONLINEAR ANALYSIS OF INTERFERING BODIES IN SUPERSONIC FLOW	5. TYPE OF REPORT & PERIOD COVERED: 17 Mar 80 - 16 May 81 FINAL
	6. PERFORMING ORG. REPORT NUMBER
7. AUTHOR(s): FRANK MARCONI	8. CONTRACT OR GRANT NUMBER(s): F49620-80-C-0044
9. PERFORMING ORGANIZATION NAME AND ADDRESS: GRUMMAN AEROSPACE CORPORATION BETHPAGE, NY 11714	10. PROGRAM ELEMENT, PROJECT, TASK AREA & WORK UNIT NUMBERS: 61102F 2307/A1
11. CONTROLLING OFFICE NAME AND ADDRESS: AIR FORCE OFFICE OF SCIENTIFIC RESEARCH/NA BOLLING AIR FORCE BASE, DC 20332	12. REPORT DATE: Jul 81
	13. NUMBER OF PAGES: 61
14. MONITORING AGENCY NAME & ADDRESS (if different from Controlling Office)	15. SECURITY CLASS. (of this report): UNCLASSIFIED
	15a. DECLASSIFICATION DOWNGRADING SCHEDULE

16. DISTRIBUTION STATEMENT (of this Report)

Approved for public release; distribution unlimited

17. DISTRIBUTION STATEMENT (of the abstract entered in Block 20, if different from Report)

18. SUPPLEMENTARY NOTES

19. KEY WORDS (Continue on reverse side if necessary and identify by block number)

FLUID MECHANICS
SUPERSONIC FLOWS
SHOCK WAVES
THREE-DIMENSIONAL FLOWS
INTERFERENCE FLOWS
NUMERICAL TECHNIQUES
STORE SEPARATION

20. ABSTRACT (Continue on reverse side if necessary and identify by block number)

This report describes a study of the flow field about interfering bodies in a supersonic stream and is directed toward the prediction of supersonic store carriage/separation. The development of computational techniques aimed at producing a usable code is disccused. The code includes a characteristic based finite difference scheme to solve Euler's equations and a new and general shock fitting scheme. One problem uncovered during this first years effort is that of transition from a regular reflection to a Mach disc shock configuration. The basic finite difference scheme has been exercised extensively and was →

DD FORM 1 JAN 73 1473 EDITION OF 1 NOV 65 IS OBSOLETE

UNCLASSIFIED

SECURITY CLASSIFICATION OF THIS PAGE (When Data Entered)

proven sound. More importantly the new shock fitting scheme is able to predict complex interactive shock patterns.

Grumman Research Department Report RE-631

NONLINEAR ANALYSIS OF INTERFERING BODIES IN SUPERSONIC FLOW

Final Report on Contract F49620-80-C-0044
for Period 17 March 1980 - 16 May 1981

for

Air Force Office of Scientific Research
Bolling Air Force Base
Washington, DC 10332

July 1981

Approved by: John T. Gramman
for Richard A. Scheuing
Director of Research

AIR FO[illegible] (AFSC)
[illegible]
This t[illegible] is
[illegible] 1-12.
Distrib[illegible]
MATTHEW J. [illegible]
Chief, Technical Information Division

ABSTRACT

This report describes a study of the flow field about interfering bodies in a supersonic stream and is directed toward the prediction of supersonic store carriage/separation. The development of computational techniques aimed at producing a usable code is discussed. The code includes a characteristic based finite difference scheme to solve Euler's equations and a new and general shock fitting scheme. One problem uncovered during this first years effort is that of transition from a regular reflection to a Mach disc shock configuration. The basic finite difference scheme has been exercised extensively and was proven sound. More importantly the new shock fitting scheme is able to predict complex interactive shock patterns.

TABLE OF CONTENTS

LIST OF ILLUSTRATIONS

I. INTRODUCTION

The study of multiple interfering bodies in high speed flow is important to the development of a number of vehicles. This report is concerned with the types of interference flow fields that will be encountered when a supersonic aircraft carries stores externally (Fig. 1). The question of the feasibility of store external carriage for a supersonic cruise aircraft is an important one to the Air Force. Internal store carriage has the penalties of increasing aircraft volume and store separation problems, while external carriage has the penalties of increased drag in addition to store separation difficulties. In order to separate a store from an aircraft, safely detailed knowledge of the forces and moments on the store are required during the entire separation process. The flow field adjusts so quickly during separation that a steady state computation at each instant of the process can predict the forces on the store very accurately, the unsteady fluid mechanics being negligible. The present effort is intended to study the fluid mechanics of a store in close proximity to an aircraft, thereby gaining insight into the feasibility of external store carriage and separation at supersonic speeds.

Current methodology requires extensive wind tunnel testing of specific aircraft store combinations. In order to evaluate aerodynamic concepts such as store shape, store control and aircraft concavity tailoring cost effectively, accurate and efficient computational tools need to be developed. The viscous effects at the Mach numbers and Reynolds numbers considered here are confined to the boundary layers (Ref 1) on the store and aircraft. Therefore an inviscid calculation can predict the interactive forces accurately. This report deals with the numerical evaluation of the inviscid moderately supersonic ($M_\infty \sim 2$) flow about simple stores and reflection planes.

Calculations which rely on the small perturbation assumption (linearized theory) may be misleading (see Section II). The fluid mechanics of a store in close proximity to an aircraft is dominated by the reflection of a shock system which requires a detailed nonlinear calculation for reliable prediction. For this reason solutions to Euler's equations are sought. The possibility of computing the complex shock system of the flow field with no special provisions (i.e., "capturing" the shocks) was considered early in this

work but because of the importance of an accurate prediction of these shocks this possibility was rejected (see Section III). Currently, the stores considered are axisymmetric and the portion of the aircraft adjacent to the store is assumed planar.

The numerical procedure used employs a conformal mapping to develop a computational grid. The mapping clusters grid points in important areas of the flow in addition to eliminating topological problems associated with the geometries under consideration (see Section IV). The finite difference scheme used is a characteristic based scheme developed by Moretti (Ref 2). The scheme is refered to as the "λ-scheme" and is discussed in Section V of this report. The scheme closely couples the physical and numerical domains of dependence of each point in the flow field thereby enhancing stability and accuracy.

The shock/contact system produced by the interaction of an axisymmetric body and a flat plate is quite complex (Fig. 2). The shock fitting scheme developed by the author for external flow fields (Ref 3 and 4) is not general enough to handle these complex shock patterns. A more powerful "shock between mesh point" scheme had to be developed and is presented in detail in Section VI. It is currently believed that no special treatment of contact surfaces needs to be developed. The weak contact surfaces which occur at the Mach numbers considered here ($M_\infty \sim 2$) can be captured adequately by the finite difference scheme used.

The sketch of Fig. 2 shows a cross section with the undisturbed axisymmetric shock ($z = 2$). The shock reflects off the wall ($z = 3$) in a "regular" manner. The term regular reflection refers to the conditions at the point where the shock meets the wall. As the computation proceeds down stream the conditions at the intersection point change so that a regular reflection can no longer be maintained. From this point on the shock reflection becomes a "Mach" reflection ($z = 4$). The regular and Mach reflections are similar to those encountered in two-dimensional flow except that the flow remains supersonic behind the Mach reflection in the three-dimensional case. The details of both these shock reflections and the transition from one to the other are discussed in Section VIII of this report. The remainder of the cross-sections sketched in Fig. 2 show how the shock system continues to develop. Section IX presents a sample calculation demonstrating the overall

soundness of the computational procedure employed. Finally, in Section X of this report the conclusions and future directions of this work are outlined.

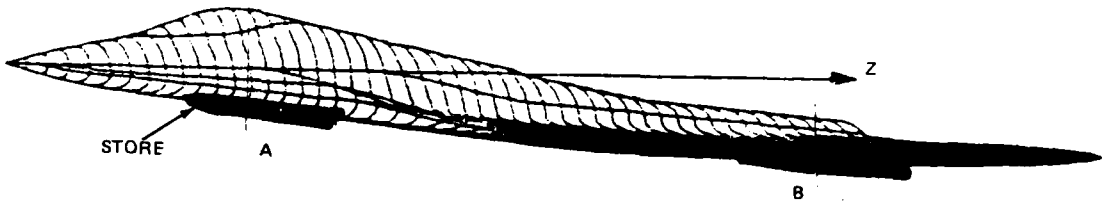

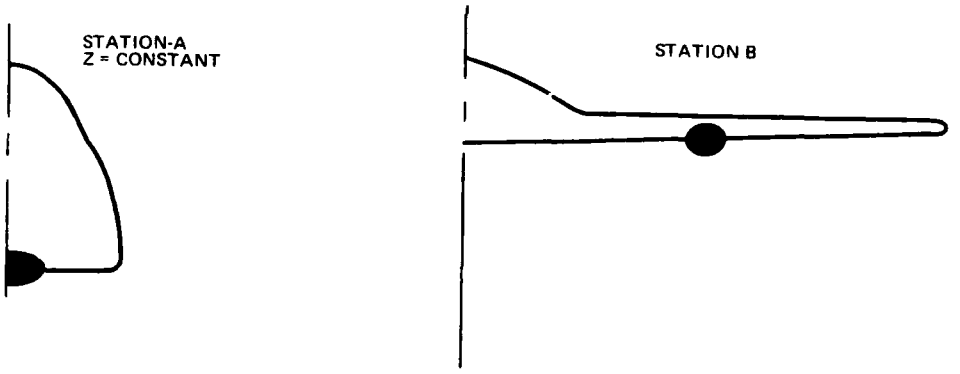

1261-001(T)

Fig. 1 Supersonic Aircraft with External Store

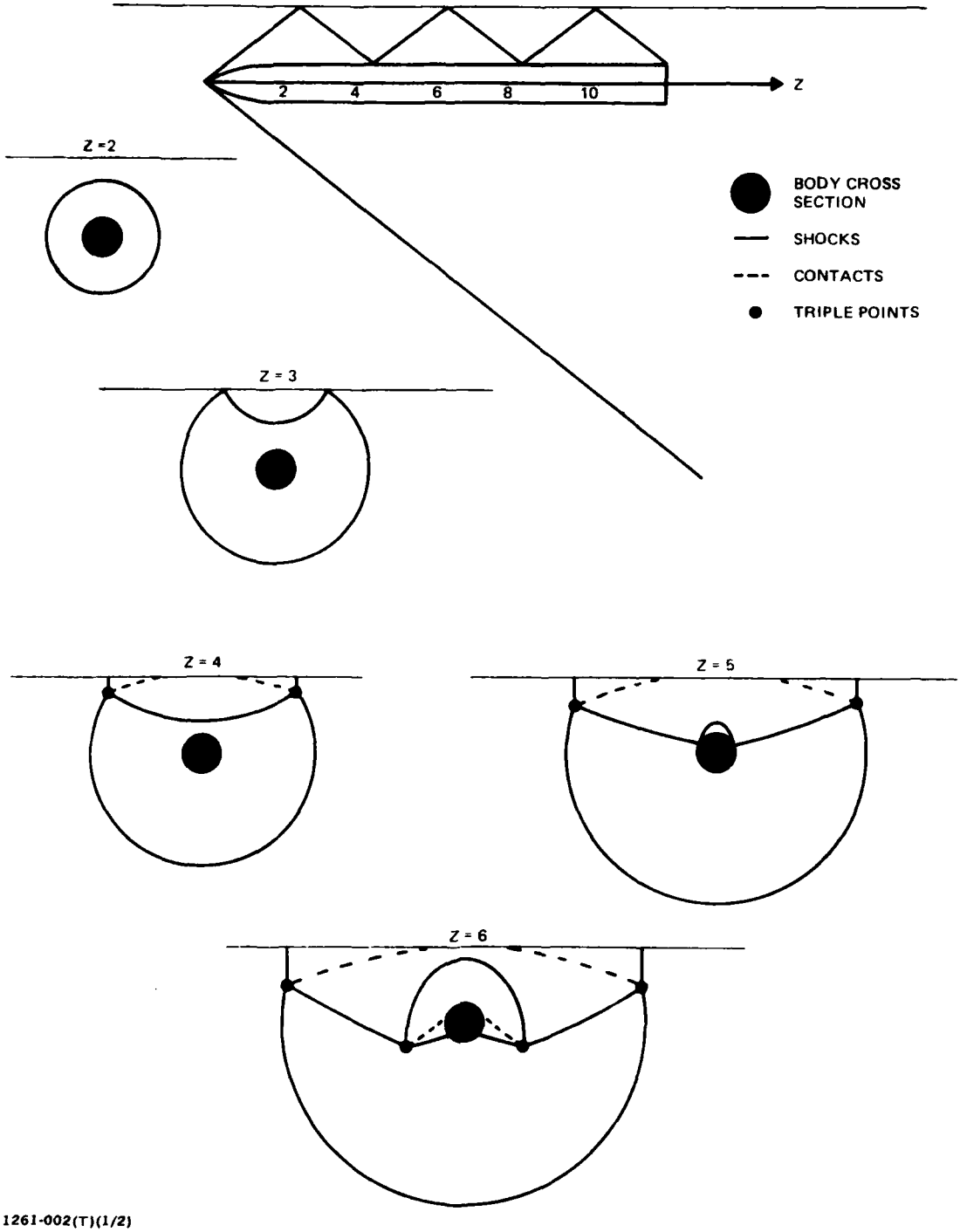

1261-002(T)(1/2)

Fig. 2 Sketch of Three-Dimenional Shock/Contact System. (Sheet 1 of 2)

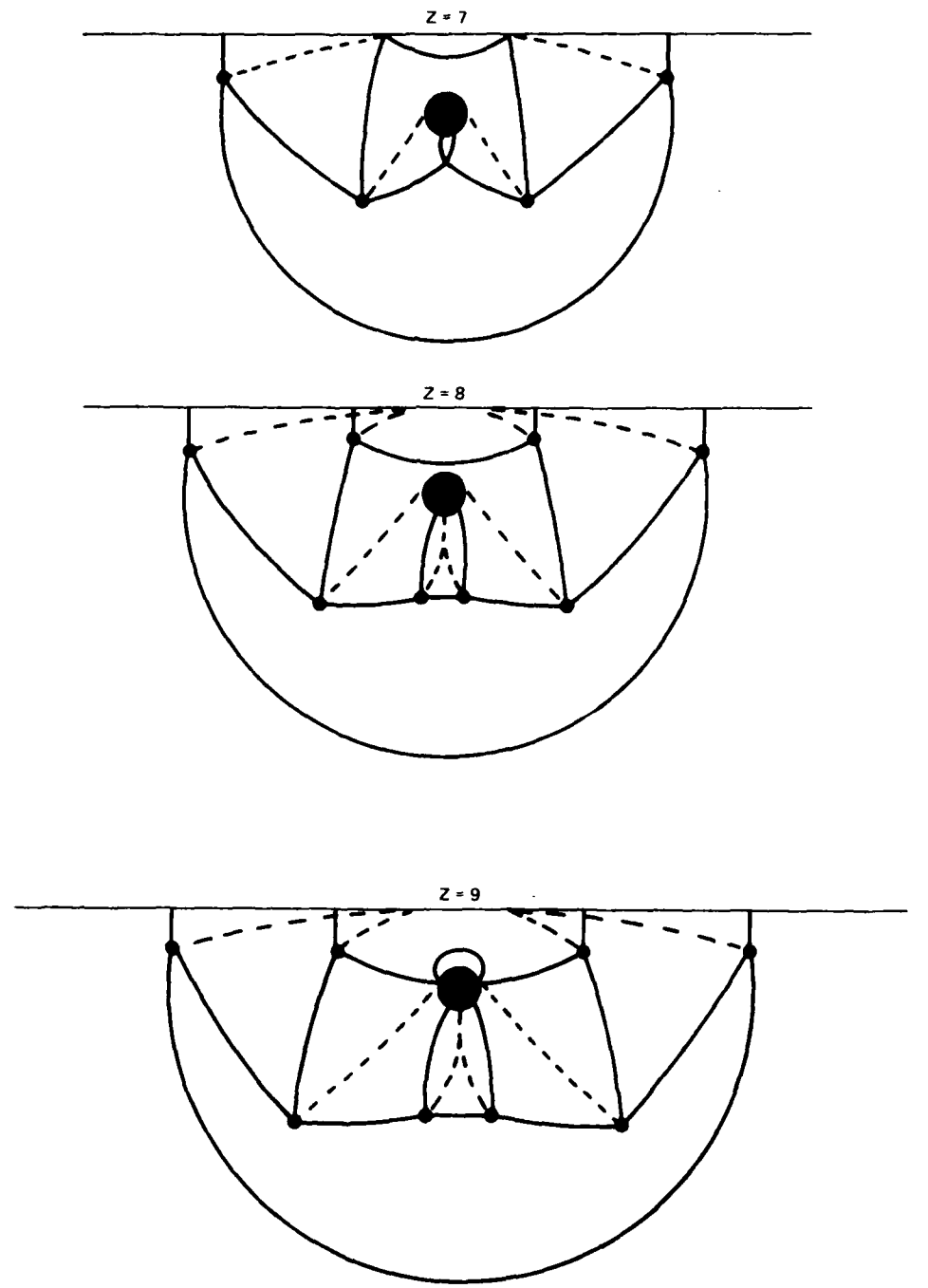

1261-002(T)(2/2)

Fig. 2 Sketch of *Three-Dimensional* Shock/Contact System (Sheet 2 of 2)

II. THE ISSUE OF NONLINEARITY

The Mach number range to be considered in this work is compatible with that of linearized theory, and the store geometries presently under consideration are slender enough to introduce only small perturbations into the flow field. However, the mutually interactive flow produced by a slender store in close proximity to a wing or fuselage exhibits nonlinear behavior due to the breakdown of the small perturbation assumption.

As an example of the breakdown of the small perturbation assumption on which linearized theory is based a two-dimensional flow is considered. Figure 3 depicts a slender two dimensional store in close proximity to a plate; also shown is the nonlinear shock pattern computed using a code developed by Salas (Ref 5). Figure 4 shows a comparison of the computed pressures on the upper surface of the store for $M_\infty = 2$ and separation distance $D/L = 0.1$ (close proximity). The figure shows the surface pressures computed with the nonlinear code and those computed with three variations of the linear results. The first (linear 1) is the standard linear theory, $C_p = -2\ u/V$ and the boundary conditions applied at $y = 0$. In the second (linear 2), C_p is computed using velocities computed by linear theory and Bernoulli's equation and the boundary conditions applied at $y = 0$. The figure shows an improvement in the pressure levels but the wave reflections occur at the wrong positions on the body. The last linear result shown (linear 3) was computed by applying the body boundary condition on the body itself, thus reflecting the down running waves from the store instead of the axis ($y = 0$). Linear 3 is typical of the results expected from a "panel method" calculation. The last linear results (linear 3) differ from the exact nonlinear result substantially. The fact is that the nonlinear computation predicts the spread of the expansion which originates near the store nose, while all the linear computations imply that all waves are parallel, so that the linear pressure returns to the free stream value periodically while the nonlinear result does not.

The result of the discrepancy between the linear and nonlinear pressure distribution on the normal force and moment acting on the store for various separation distances is shown in Figs. 5 and 6. The difference in the predicted force and moment is very large; these discrepancies will have a significant impact on the design of reliable store separation/carriage

systems. While the results shown here are for two-dimensional flows and small separation distances the same types of trends could be expected in the three-dimensional flow. Three-dimensional effects will tend to reduce the nonlinearity of these flow fields, but it seems that a computation based on the small perturbation assumption will have difficulty dealing with wave reflections since these waves are not significantly reduced in strength as the computation proceeds downstream. The shock reflections dominate these interactive flow fields and the sensitivity of the critical parameter C_M (pitching moment) to the location of these waves indicates that the question of nonlinearity is an important one. The results of this study indicate that solutions to Euler's equations are required for the accurate prediction of the forces on the store.

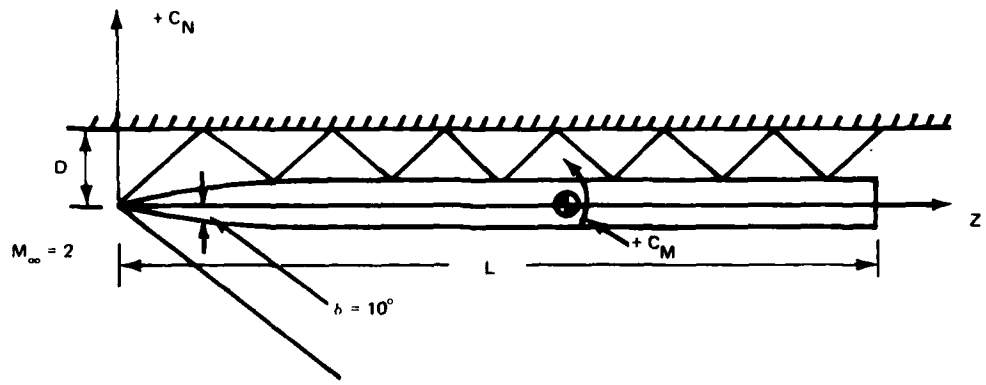

1261-003(T)

Fig. 3 Two-Dimensional Body and Shock System

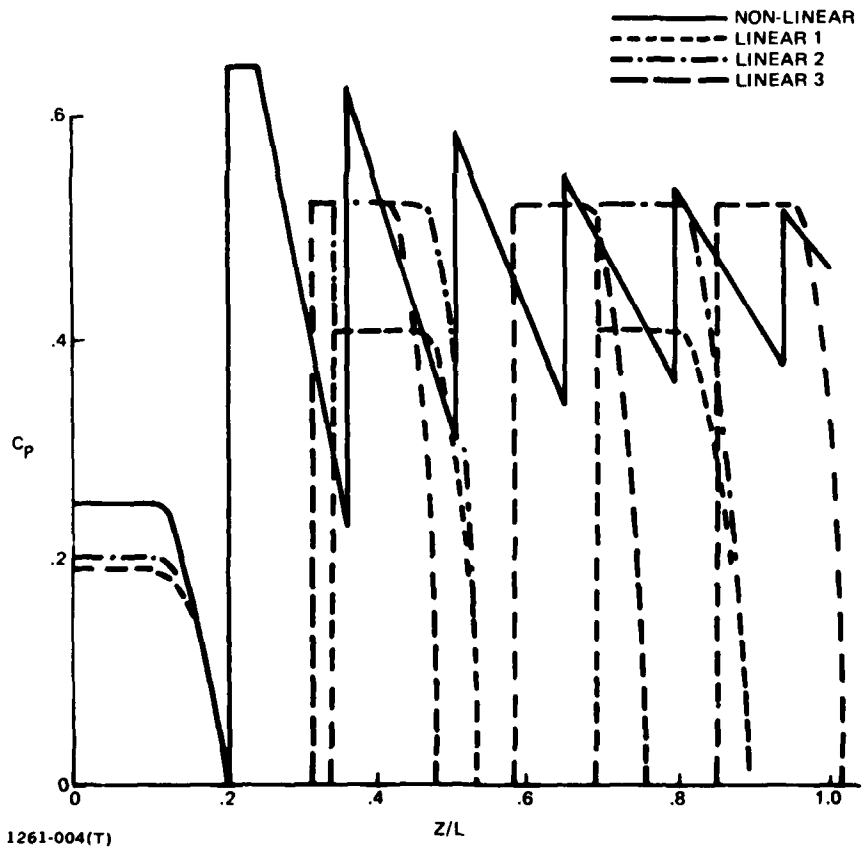

1261-004(T)

Fig. 4 Store Top Surface Pressure Comparison

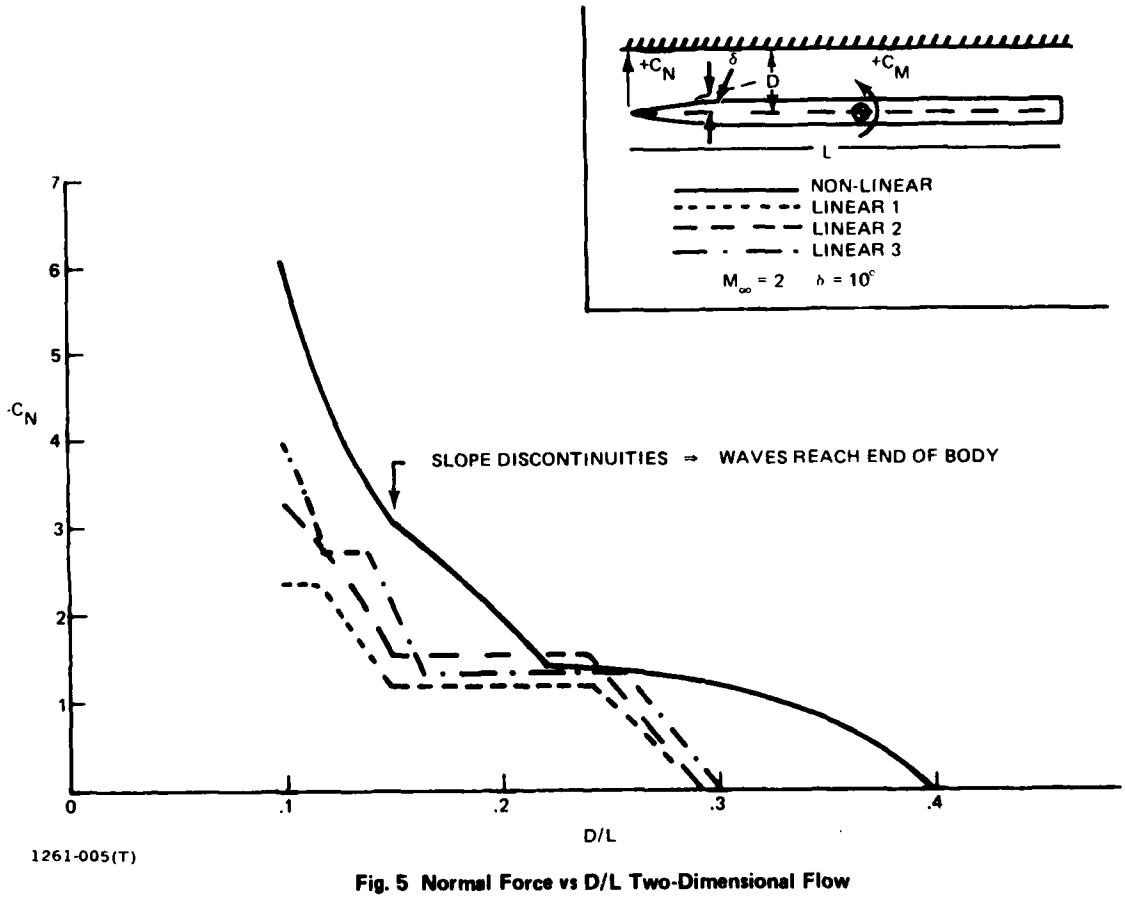

Fig. 5 Normal Force vs D/L Two-Dimensional Flow

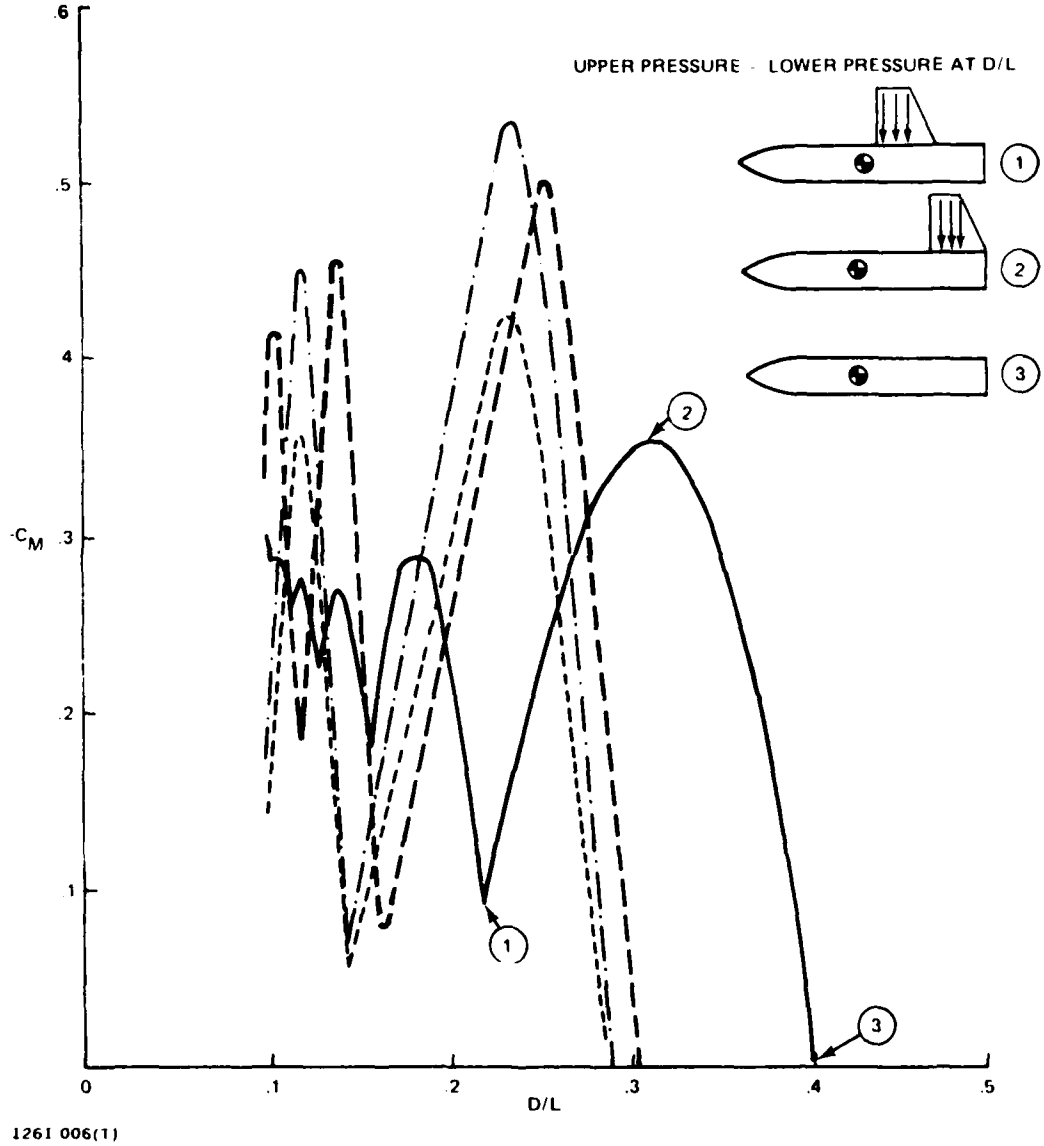

Fig. 6 Moment vs D/L Two-Dimensional Calculation

III. THE ISSUE OF SHOCK CAPTURING

The possibility of using a finite difference scheme which handles shock waves automatically (i.e., captures shock waves) is always attractive in supersonic flow. In the present problem this is particularly true in light of the very complex shock patterns. A number of shock capturing schemes were studied ranging from the early work of Kutler (Ref 6) to the more recent work of Steger (Ref 7) and that of Grossman (Ref 8). In addition the possibility of capturing the shocks using Moretti's λ-scheme was investigated. These studies were conducted using the two-dimensional wedge flow as a model problem. The results are shown in Fig. 7.

Figure 7a depicts the pressure distribution from the wedge surface through a shock computed using the full potential (non-conservative) solution technique of Ref 8. The exact Euler solution also appears in the figure. This procedure uses the upwind differencing scheme applied by Jameson (Ref 9) so successfully to transonic airfoil problems. It is believed that the large overshoot on the higher pressure side of the shock in Fig. 7a is due to the fact that the shock considered here is oblique and the flow on either side of the shock is supersonic. A coordinate system can be chosen such that one component of velocity transitions from supersonic to subsonic across the shock as was done in Ref 8. When the shock reflects and changes family (from uprunning to downrunning) the transonic shock condition is violated again and the pressure distributions become those of Fig. 7a. The interaction problem under consideration here is dominated by reflected shocks and therefore one cannot tailor a coordinate system to capture shocks.

Figures 7b and 7c show the computed results using the standard Strong Conservative Formulation of Euler's Equations (Ref 6) compared with the exact solution. The finite difference scheme used in these computations is due to MacCormack (Ref 10). The results of Fig. 7b look quite good, but are misleading. It turns out that this scheme is very sensitive to the marching stepsize used. The finite difference scheme is an explicit marching scheme and therefore must satisfy the standard Courant-Friedricks-Lewy (C.F.L.) stability condition. Simply stated $\Delta z = (C_n \Delta y/\lambda)_{min}$ where λ is the characteristic slope and C_n is the Courant number. The subscript min

implies the minimum value throughout the flow field. The Courant number is less than unity for stability. The results of Fig. 7b are computed with a local Courant number of .9 while the results of Fig. 7c are computed with a Courant number of .5. The deterioration of the results is quite significant. In any nonuniform flow field it is very difficult to use a marching step such that the Courant number at the shock is close to one. In particular for the problem under consideration (with the number of shocks present in each cross section) it would be impossible to maintain a Courant number near .9 at all the shocks. For this reason the results of Fig. 7c can be considered typical for the Standard Conservation Law formulation.

The results using the Conservation Law Form Flux Vector Splitting of Ref 7 are shown in Fig. 7d. This scheme is independent of Courant number but exhibits a large undershoot on the low pressure side of the shock. This scheme utilizes characteristic based differencing in conjunction with Euler's equation in conservative form. Here again the results are somewhat disappointing.

The last scheme tested was Moretti's λ-scheme. The scheme is non-conservative so that captured shocks exhibit an incorrect slope and ultimately move to the wrong position. This scheme is not intended to capture shocks but was developed to remain stable in the presence of shock waves and to be used in junction with a sound shock fitting scheme. None of the results of Fig. 7 are considered acceptable, particularly because the interference problem considered here is totally dominated by shock waves and their reflections. It would be possible to use the conservative schemes of Ref 6 and 7 to obtain a qualitative picture of the shock system for the store separation problem but any quantitative results would be questionable. For this reason a shock fitting scheme must be used.

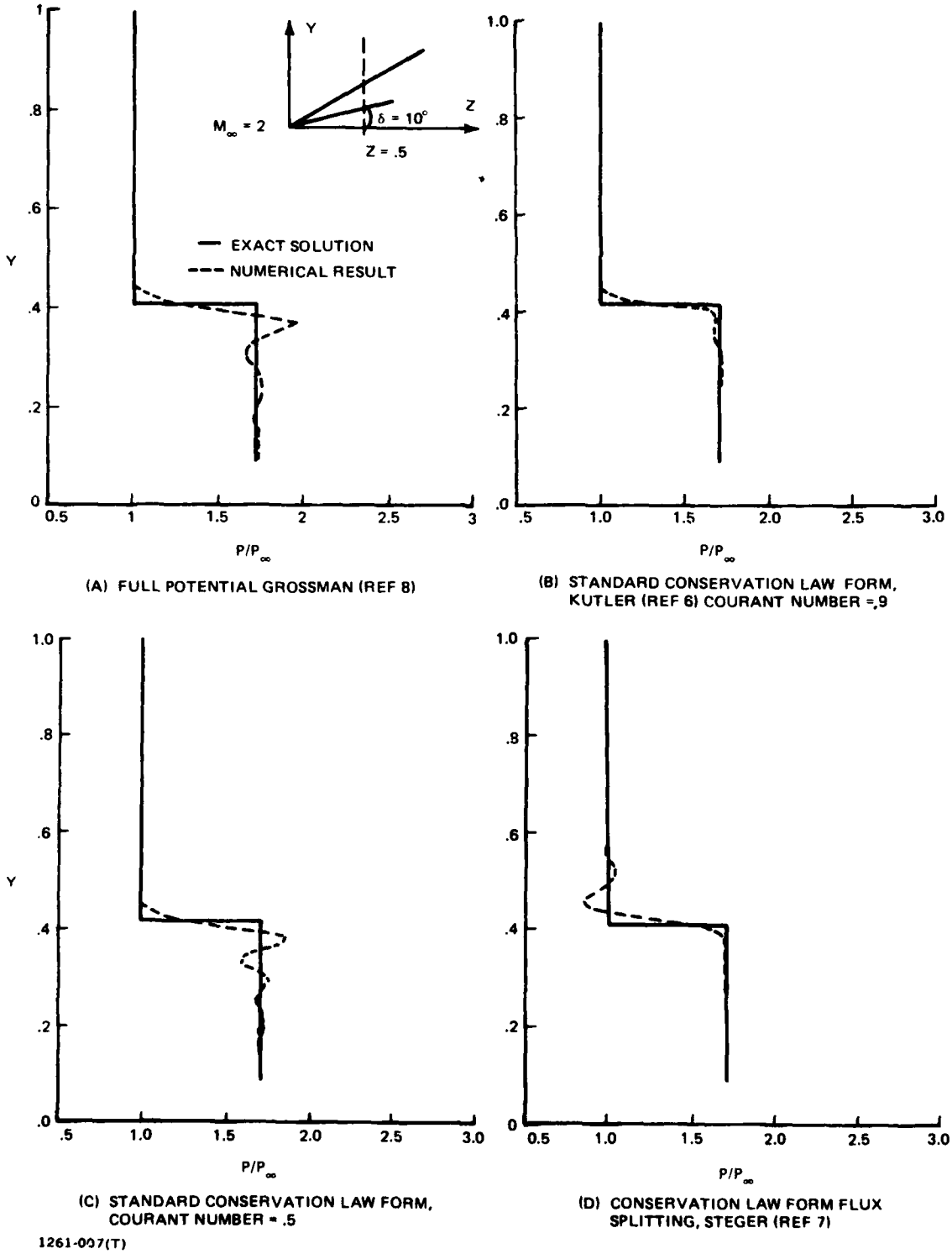

(A) FULL POTENTIAL GROSSMAN (REF 8)

(B) STANDARD CONSERVATION LAW FORM, KUTLER (REF 6) COURANT NUMBER =.9

(C) STANDARD CONSERVATION LAW FORM, COURANT NUMBER = .5

(D) CONSERVATION LAW FORM FLUX SPLITTING, STEGER (REF 7)

1261-007(T)

Fig. 7 Captured Shock Pressure Distributions, 50 Points Between Wall and Y = 1

IV. DEVELOPMENT OF A COMPUTATIONAL GRID

The choice of a computational grid is a critical step in the development of any computational tool; this is especially true in the case of nonlinear tools. The flow fields under consideration here are of an interactive nature; this fact was taken into account when the computational grid was being devised. It was noted that the supersonic flow about a store/plate combination involved a wave system propagating into an undisturbed store flow field. Consider, for example, Fig. 8, which shows (shaded area) the region of the flow field which is unaffected by the presence of the plate (i.e., undisturbed store flow). Because of the large extent on this undisturbed store flow field it is worthwhile computing this region with a coordinate system dedicated to the store. For example, if the store is circular in cross section a polar coordinate system is used; in addition, if the store axis is aligned with the free stream velocity its undisturbed flow is axisymmetric and a great deal of computational time is saved by computing one meridional plane.

The shock wave moving from the plate into the undisturbed store flow field is the reflected store nose shock (front shock, Fig. 8) and the conditions on its low pressure side are interpolated from the store grid using a second-order scheme. The flow properties on either side of this shock are computed simultaneously. Both computations have the same marching direction, and the step size is taken as the minimum of that needed in each region, so that interpolation is necessary only in each cross section. The use of this concept makes the choice of a computational grid a bit easier, since the store flow is computed with a grid adapted to its shape.

In order to compute the flow behind the front shock (Fig. 8) it is important that a coordinate system is used in which both the plate and store are coordinate surfaces. This is true because the computational logic involved in applying the boundary conditions become simpler, but more importantly because the flow field gradients are usually smaller in such a coordinate system. An additional consideration in the development of a coordinate system is that shocks are simply defined with respect to it.

In the present work two mappings have been considered. The first maps the region exterior to the store and plate to the region exterior to a circular arc slit and a plate. The transformation is produced by the series of mappings shown in Fig. 9. The last of these mappings involves an infinite series. Although this series can be truncated after only five terms it is a time consuming process. An adequate computational grid is achieved by using a simple bilinear mapping. This mapping is much simpler to apply and maps the region between the store and plate to the region in the annulus; i.e., the W_1 plane of Fig. 9. The grids generated using these two mappings are shown in Figs. 10a and 10b. The simpler mapping satisfies all the requirements mentioned previously and was the one ultimately used.

With the marching direction z taken along the plate and parallel to the axis of the store the transformation to the final computational plane is as follows. Let the complex variable $W_0 = x + iy$, the conformal mapping yields $W_1 = re^{i\theta} = R_1(1+iW_0/\beta)/(i+W_0/\beta)$ and the marching direction is unchanged ($z = z$). The coordinates in the mapped space are then (r,θ,z) a polar system centered about the store axis. All dimensions are normalized with respect to the separation distance (the vertical distance between the store axis and plate). The radius of the store in the mapped space is unity while the plate is transformed to a circle of radius $R_1=(1+\sqrt{1-R_s^2})/R_s$. The coefficient of the mapping $\beta = (R_1^2-1)/(R_1^2+1)$. R_s is the radius of the store in the physical space. The final computational space is generated by normalizing the mapped space in the radial direction

$$X = (r-R_0)/(R_1-R_0) = (r-1)/(R_1-1)$$

$$Y = \theta$$

$$Z = z$$

The derivatives of these transformations are required to transform the governing equations and are evaluated by chain rule differentiation.

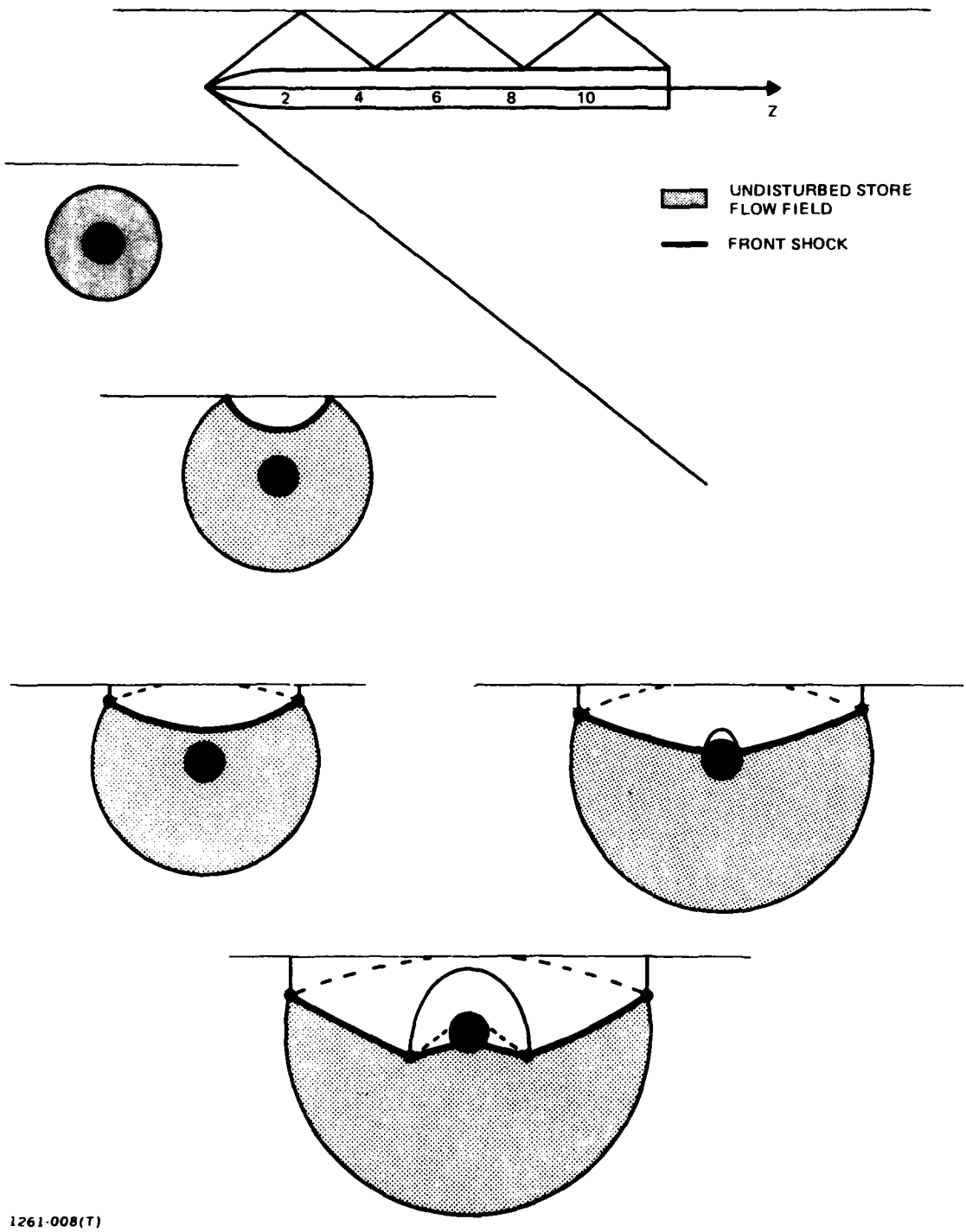

Fig. 8 Three-Dimensional Store Flow Indicating Undisturbed Store Flow

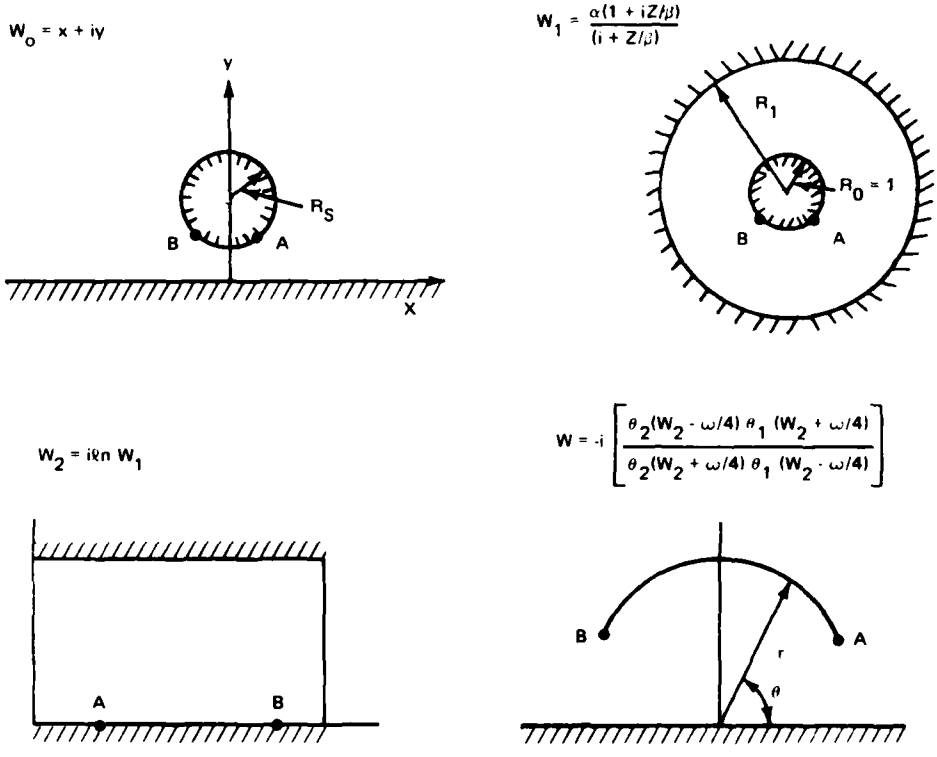

$$\text{WHERE } \theta_1(z) = 2q^{1/4} \sum_{n=0}^{\infty} (-1)^n q^{n(n+1)} \sin(2n+1)\, z$$

$$\theta_1(z) = 2q^{1/4} \sum_{n=0}^{\infty} q^{n(n+1)} \cos(2n+1)\, z$$

$$\text{AND } q = e^{i\omega}$$

1261-009(T)

Fig. 9 Series of Conformal Mappings

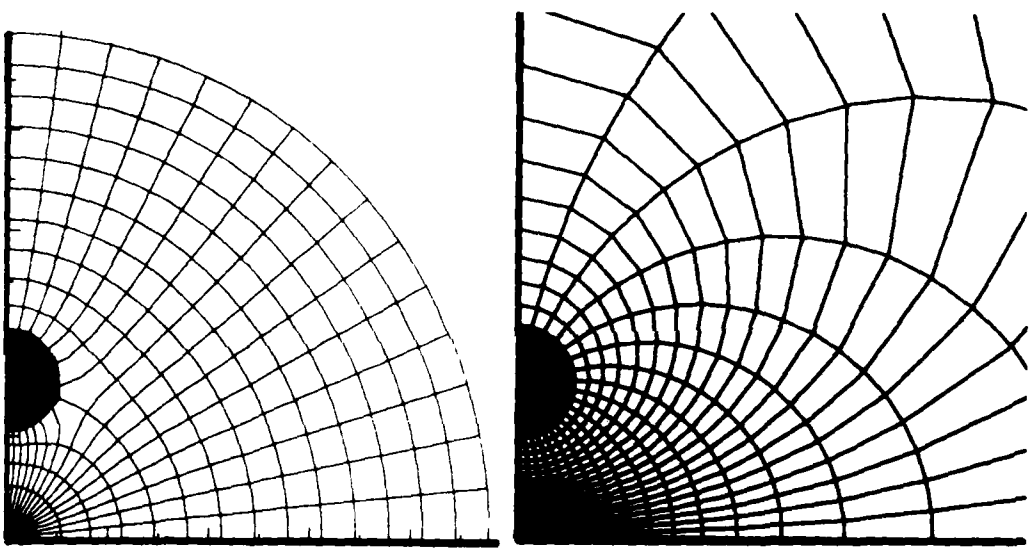

(A) COMPLEX MAPPING

(B) SIMPLE BILINEAR MAPPING

1261-010(T)

Fig. 10 Computational Grids

V. CHARACTERISTIC BASED FINITE DIFFERENCE SCHEME

The finite difference scheme used here is the predictor-corrector, characteristic based scheme presented by Moretti in Ref 2. The scheme is a second order explicit marching scheme which is stable for a marching step $\Delta Z \leq (\Delta X/2\lambda_i^x, \Delta Y/2\lambda_i^y)_{min}$ for i = 1,2,3. The subscript min implies the minimum values over the entire flow field at each marching step. The intervals in the final computational plane (see Section IV) are ΔX and ΔY and λ_i^x and λ_i^y are the bicharacteristics in the X - Z and Y - Z planes, respectively. The basic concept underlying the scheme is to take one sided differences in the X and Y directions depending on the characteristic slopes λ_i^x and λ_i^y. Using this procedure closely couples the physical and numerical domains of dependence of each point in the flow field thereby leading to a stable and physically realistic solution. The only limitation on this procedure is that the Mach number component in the marching direction must be supersonic, which is true of any marching technique.

The equations considered here are Euler's equations written in primitive variables for the Cartesian coordinates of Fig. 11, these are

$$\begin{aligned} w\,P_z + \gamma w_z &= -(uP_x + vP_y + \gamma u_x + \gamma v_y) \\ w\,u_z &= -(uu_x + vu_y + T\,P_x) \\ w\,v_z &= -(uv_x + vv_y + T\,P_y) \\ TP_z + ww_z &= -(uw_x + vw_y) \\ wS_z &= -(uS_x + vS_y) \end{aligned} \tag{1}$$

where $T = \bar{T}/\bar{T}_\infty$, $P = \ln(\bar{p}/\bar{p}_\infty)$, $S = (\bar{S}-\bar{S}_\infty)/\bar{c}_v$ and all velocities are nondimensionalized with respect to $\sqrt{\bar{p}_\infty/\bar{\rho}_\infty}$ (the barred quantities are dimensional), x, y and z are nondimensionalized with respect to L defined in Fig. 11 as the distance between the plate and store. The equation of state relating temperature, pressure and entropy becomes

$$\ln T = P(\gamma-1)/ + S/\gamma \tag{2}$$

Equations 1 and 2 are a complete set of six equations for the six unknowns. All the derivatives of Eq (1) are transformed to the final computational

plane. The unknown velocity components (u,v) are replaced by $\sigma = u/w, \eta = v/w$. The equations are then combined into characteristic form. For the characteristics in the X-Z plane

$$A^X(P_Z{}^X + \lambda_1{}^X P_{X1}) + B^X(\sigma_Z{}^X + \lambda_1{}^X \sigma_{X1}) + C^X(\eta_Z{}^X + \lambda_1{}^X \eta_{X1}) = 0 \quad (a)$$

$$-A^X(P_Z{}^X + \lambda_2{}^X P_{X2}) + B^X(\sigma_Z{}^X + \lambda_2{}^X \sigma_{X2}) + C^X(\eta_Z{}^X + \lambda_2{}^X \eta_{X2}) = 0 \quad (b) \qquad (3)$$

$$D^X(P_Z{}^X + \lambda_3{}^X P_{X3}) + E^X(\sigma_Z{}^X + \lambda_3{}^X \sigma_{X3}) + F^X(\eta_Z{}^X + \lambda_3{}^X \eta_{X3}) = 0 \quad (c)$$

$$S_Z{}^X + \lambda_3{}^X S_{X3} = 0 \quad (d)$$

The coefficients A^X, B^X, C^X, D^X, E^X and F^X are functions of the mappings (for more detail see Ref 2). The coefficients $\lambda_1{}^X$ and $\lambda_2{}^X$ are the slopes of the uprunning and downrunning bicharacteristics in the X - Z plane and $\lambda_3{}^X$ is the slope of the stream line in the X - Z plane. With all the coefficients and X derivatives evaluted at the known marching plane Eq 3 (a), (b), and (c) become a set of linear equations for the unknowns $P_Z{}^X$, $\sigma_Z{}^X$ and $\eta_Z{}^X$ while Eq 3 (d) can be solved directly for $S_Z{}^X$. A similar set of equations can be written for the biocharacteristics in the Y - Z plane and the derivative $P_Z{}^Y$, $\sigma_Z{}^Y$, $\eta_Z{}^Y$, and $S_Z{}^Y$ can be computed. The total derivative in the marching direction is obtained simply by adding the contributions from the X - Z and Y - Z characteristics ($P_Z = P_Z{}^X + P_Z{}^Y$, etc.). The important step in the scheme is the evaluations of the spatial derivatives P_{Xi}, σ_{Xi}, η_{Xi} and S_{Xi} (i = 1,2,3). These derivatives are approximated by one-sided differences depending on the sign of their coefficients $\lambda_i{}^X$. In order to attain second order accuracy the scheme is divided into a predictor and corrector step. The scheme proceeds as follows

$$f_{Xi} = \begin{cases} (f_E - f_D)/\Delta X & (\lambda_i{}^X < 0) \\ (2f_D - 3f_C + f_B)/\Delta X & (\lambda_i{}^X > 0) \end{cases}$$

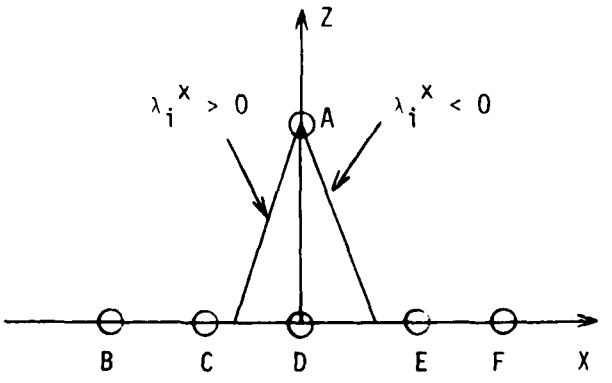

the vector f is (p, η, σ, S). The same formuli are used for f_{yi} and the predicted values are

$$\tilde{f} = f(Z) + f_Z \Delta Z$$

In the corrector step

$$\tilde{f}_{Xi} = \begin{cases} (-2\,\tilde{f}_D + 3\,\tilde{f}_E - \tilde{f}_F)/\Delta X & (\lambda_i{}^X < 0) \\ (\tilde{f}_D - \tilde{f}_C)/\Delta X & (\lambda_i{}^X > 0) \end{cases}$$

and the final updated values are

$$f(Z+\Delta Z) = (f(Z) + \tilde{f} + \tilde{f}_Z \Delta Z)/2.$$

After P, η, σ, and S are updated using this procedure the axial velocity component is computed from the energy equation in the form

$$w = \sqrt{\frac{2(H_o - \gamma/\gamma\text{-}1\ T)}{\eta^2 + \sigma^2 + 1}} \qquad (4)$$

where H_o is the free stream total enthalpy and the temperature T is computed from the equation of state (Eq 2).

As mentioned in the previous section of this report, the undisturbed store flow field is evaluated with an axisymmetric computation. This calculation also uses the λ-scheme as its basis. The axisymmetric code supplies initial conditions for the three-dimensional code, and is itself started with a Taylor-Maccoll cone solution.

In order to demonstrate the stability of this scheme, a store/ plate flow field was computed with no special provisions for the shock waves. Figure 12 shows computed cross sectional isobar for a store/plate flow field. The dashed line in the figures (Fig. 12 a - d) separates the region which was computed by assuming axisymmetric flow and that computed with a fully three-dimensional computation. The choice of this separator was somewhat arbitrary and in fact the results show that it is too far from the region affected by the presence of the plate. The results of Fig. 12 show the main features of the flow field. Figure 12b shows the shock reflecting from the plate with a regular reflection at the shock wall intersection, while figure 12c shows that this intersection has become a Mach disc as expected. Figure

12c shows a regular reflection on the surface of the store. This calculation was performed with an 80 x 80 grid in each cross section and yet the shock looked quite thick at z = 2.28 (Fig. 12c). The fitting of the shock waves in these flow fields will be discussed in Sections VII and VIII.

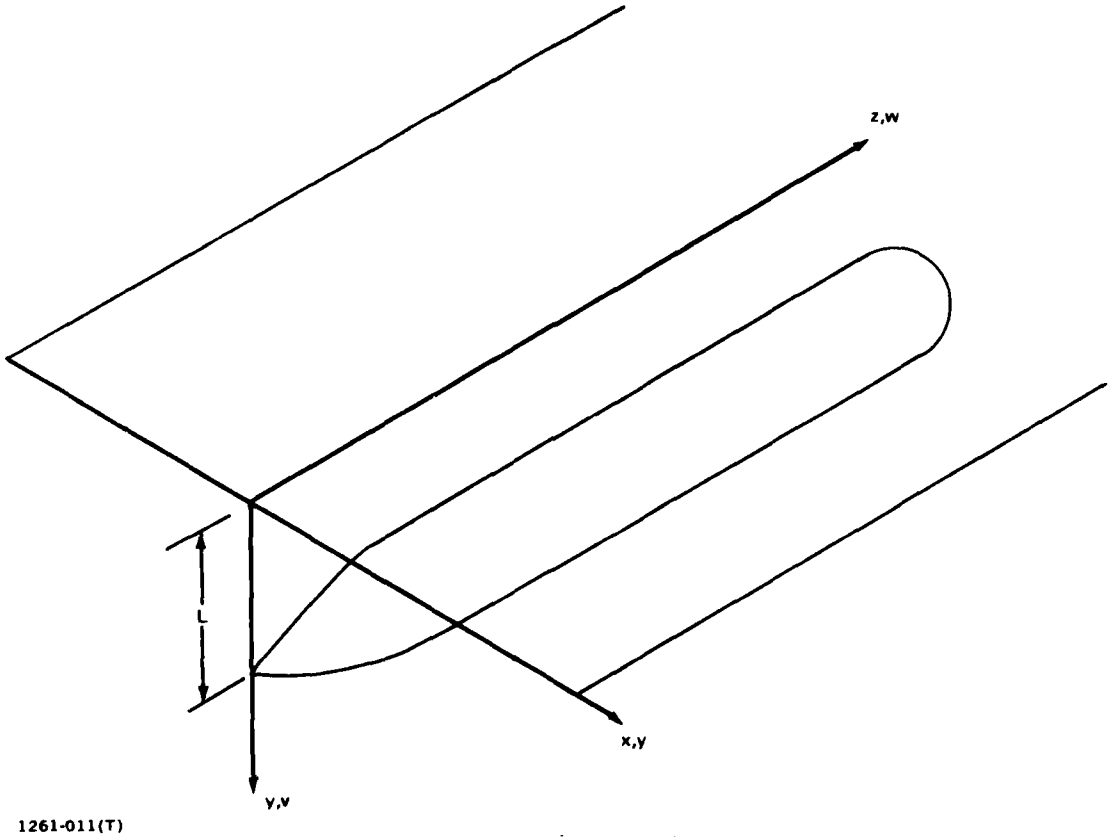

1261-011(T)

Fig. 11 Cartesian Coordinate System

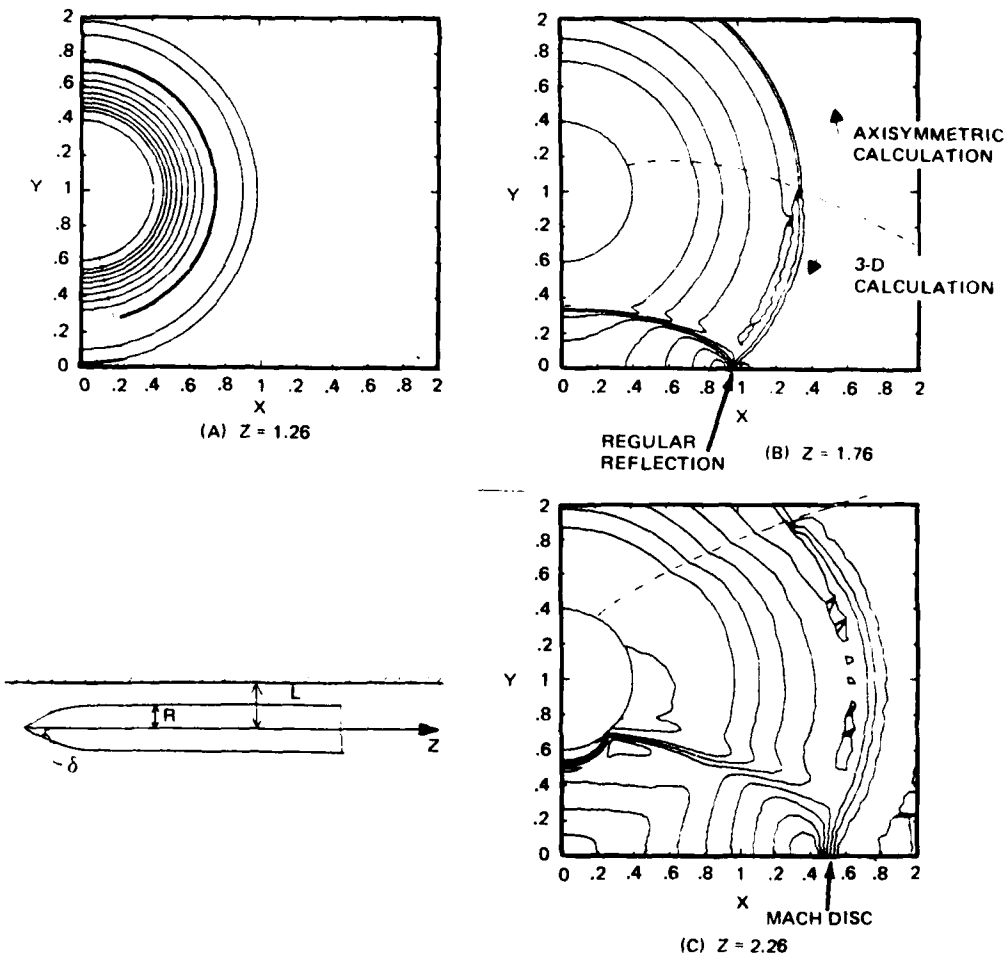

Fig. 12 Computed Isobars, Captured Shock ($M_\infty = 2, \delta = 20^\circ$, R/L = .4)

VI. SOLID BOUNDARY CONDITIONS

At the store or plate the boundary condition requires that the velocity normal to the surface must vanish. The correct procedure for applying this condition is to disregard the compatibility condition along the characteristic reaching a point from inside the surface and substituting for it the vanishing of the normal velocity. In the present work we used a procedure which is very simple and is equivalent to this condition. This procedure was developed by Abbett (Ref 11). A similar approach has been used more recently by Rudman (Ref 12) and de Neef (Ref 13).

The basic concept in the procedure is to correct the pressure and velocity slope computed by the finite difference scheme. After all the flow field variables at the grid points have been updated, using the finite difference scheme and one sided differences at the boundries, the velocity normal to the solid boundaries is not zero. A Prandtl-Meyer expansion or compression is used to turn the flow tangent to the surface and change the surface pressure accordingly. The plane in which to perform this correction is somewhat arbitrary. In the present work, the plane made up by the surface normal and marching direction is chosen. This choice yields accurate and reliable results. The correction is so small in terms of the angle through which the velocity vector is rotated that a second order expression relation pressure and flow-deflection is used instead of the full Prandtl-Meyer equations. The entropy is left as that computed from the finite difference scheme. In addition, the velocity component in the direction normal to the correction plane is left unchanged. With the fact that the normal velocity is zero the last velocity component can be computed with the energy equation (Eq 4). This procedure defines all the flow field quantities at the solid surface.

VII. TREATMENT OF SHOCK WAVES AND CONTACT SURFACES

As has been pointed out a number of times already, the shock system in supersonic store separation/carriage plays a very important role. Therefore, these shocks must be followed exactly and forced to satisfy the Rankine-Hugoniot jump conditions. The procedure whereby all discontinuities (shocks and contacts) are followed as internal boundaries of the computational plane (Ref 14 and 15) requires that all discontinuities are along mesh lines. The shock/contact pattern considered here is too complex to be followed in this manner. A more powerful procedure dubbed "floating shock fitting," introduced by Moretti (Ref 16), is used in the present work. This scheme has been applied successfully to two dimensional flows by Salas (Ref 5) and to simple three-dimensional flows by Rudman (Ref 17). In the present work the procedures of the previous investigators have been simplified and generalized.

The floating shock fitting scheme follows discontinuity surfaces allowing these surfaces to move or float between mesh points of the computational grid. Figure 13 shows the cross section in a marching plane (z = constant) of a complex shock system. The shock surface crosses grid lines in an arbitrary fashion. This is the basic concept behind the floating shock fitting scheme and is the way the procedure gains generality over the scheme of Ref 14 and 15.

In order to track the evolution of the shock system as the computation proceeds the cross sectional shock surface is defined by a number of points (shock points) and these points are followed in the marching direction. For two basic reasons the shock points are defined as the intersections of the cross sectional shock surface and all grid lines. This definition ensures that the discretized resolution of the shock is consistent with the resolution of the rest of the flow field. Consider the shock of Fig. 14; the surface is defined by six points at the initial cross section K_0. The shock is small at this station and can be defined by a small number of points. As the computation proceeds, the shock moves across the grid and at the final station shown ($K = K_3$) is much longer and has 15 points defining it. The addition of shock points is done in a natural fashion as is shown at the two intermediate stations of Fig. 14. The second reason for defining shock points

at all shock surface grid line intersections is one of convenience. One of the basic concepts in shock fitting is to avoid differencing across the shock. With shock points defined at all shock grid line intersections it is a simple matter to decide which grid points are adjacent to the shock and therefore to decide which differences to avoid. Each grid point has two indicies ($IX_{i,j}$ and $IY_{i,j}$) associated with it, if a shock point is in the mesh interval to the right or left of the mesh point i,j the index $IX_{i,j} = \pm 1$, respectively. If no shock point is in an adjacent interval $IX_{i,j} = 0$. $IY_{i,j}$ indicates shock points above or below a mesh point. If $IX_{i,j} \neq 0$ the X differences of Eq 3 are taken one sided to avoid the shock.

The computer code logic, which assures that there are, at each cross section, shock points at each shock surface grid line intersection, is quite complex. This is because of the addition and subtraction of shock points as the shock crosses over grid points. In the present work, the computational grid and shock systems considered assures that there will be one shock point on every Y = constant line (see Fig. 13). This fact makes it simple to locate new shock points on these lines. The procedure is to simply locate the maximum pressure gradient on each Y = constant line and locate a new shock point by interpolating between existing shock points. Once all of these points are located new points on the X = constant lines are located by interpolating between existing shock points. Any gaps in the shock are filled.

As alluded to in the previous paragraph, the shock points are divided into two types. The points on Y = constant lines (X-type) and points on X = constant line (Y-type) (see Fig. 15). The shock point calculation revolves around computing X_{SZ} (the slope of the shock in X-Z plane) for X-type shock points and Y_{SZ} for Y-type shock points. With these quantities it is a simple matter to update the shock point locations from one marching plane to the next. The first step in the shock point computation is to evaluate the slope of the shock in cross section, X_{SY} for X-type shocks and Y_{SX} for Y-type shocks. This is done using finite differences and the given shock point locations in the current Z = constant plane. The difference, scheme used is second order and involves the shock points immediately adjacent to the point under consideration. Difficulties arise because shock points can become too close to each other when a shock approaches a grid point. Under these

circumstances differences can not be taken between two adjacent shock points because the interval becomes too small. In this case the next adjacent shock point is used. The question of how close is close is currently causing minor wiggles in the shock, this problem will be solved shortly.

Once the cross slopes X_{SY} and Y_{SY} are evaluated the slopes X_{SZ} and Y_{SZ} can be computed by satifying the Rankine-Hugoniot conditions and the compatibility conditions along a characteristic reaching the shock from the high pressure side. The flow field conditions on the low pressure side of the shock are evaluated by extrapolating from the adjacent grid points. The computation of the conditions on the high pressure side of the shock is simplified using a procedure developed by deNeef (Ref 13); a similar scheme was developed independently by Rudman (Ref 12). The procedure starts by guessing the shock slope in the marching direction (X_{SZ} or Y_{SZ}) and evaluating the normal to the shock with the computed cross slope (X_{SY} or Y_{SX}). With the normal to the shock it is a simple matter to compute the flow field conditions on the high pressure side of the shock from the Rankine-Hugoniot jump relations. The contribution of deNeef is to write the compatibility condition along a characteristic reaching the shock in the form

$$A(P_{FD}-P_{RH}) + B(\sigma_{FD} - \sigma_{RH}) + C(\eta_{FD} - \eta_{RH}) = 0 \qquad (5)$$

The subscripts FD imply values computed from the finite difference scheme and RH values computed from the Rankine-Hugoniot relations and the guested shock slope. The coefficients A, B, C are those of Eq 3a or b ($\pm A^X$, B^X and C^X) depending whether the characteristic reaching the shock is right or left running. This is true for X-type shocks where the characteristic taken is in the X-Z plane, for Y-type shocks the chosen characteristic is the one in the Y-Z plane. The shock slope X_{SZ} is iterated until Eq (5) is satisfied exactly. The flow field variables P_{FD}, σ_{FD}, and η_{FD} are extrapolated from adjacent grid points. Once the iteration converges the shock values P_{RH}, σ_{RH}, η_{RH}, S_{RH} (the entropy behind the shock) are used to correct the grid point closest to the shock.

This procedure can be used for contact surfaces if the Rankine-Hugoniot conditions are exchanged for appropriate contact boundary conditions. The conditions at three-dimensional contact surfaces are discussed in detail

in Ref 15. At the Mach numbers considered here, the jumps in entropy and tangential velocity across a contact surface are small; also the λ-scheme has the capability of capturing contacts. No special treatment for contact surfaces is expected to be necessary except at the point where the regular reflection transitions to a Mach disc. This issue is discussed in the next section.

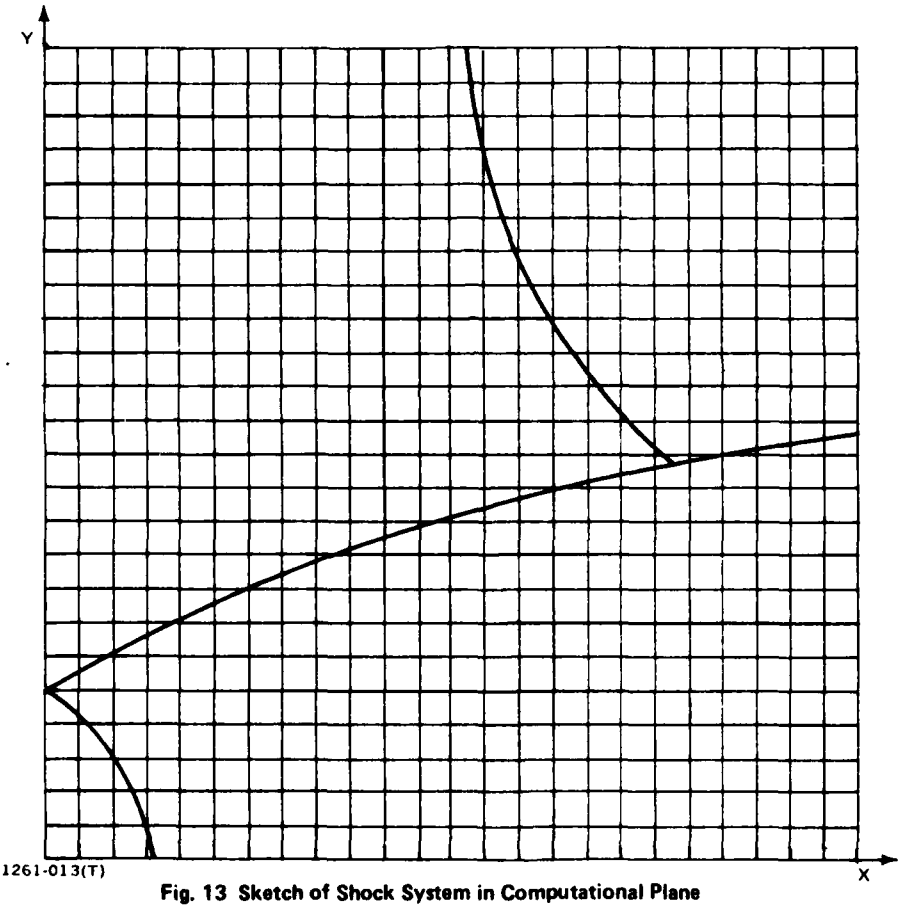

Fig. 13 Sketch of Shock System in Computational Plane

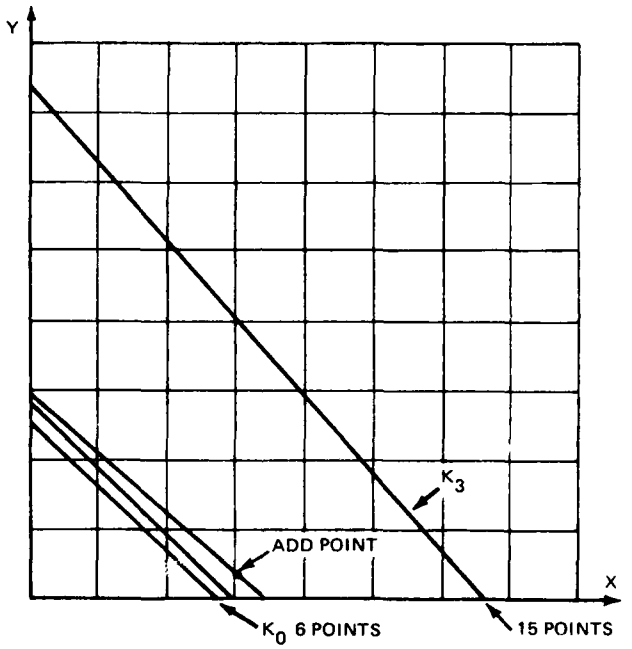

1261-014(T)

Fig. 14 Automatic Shock Point Addition

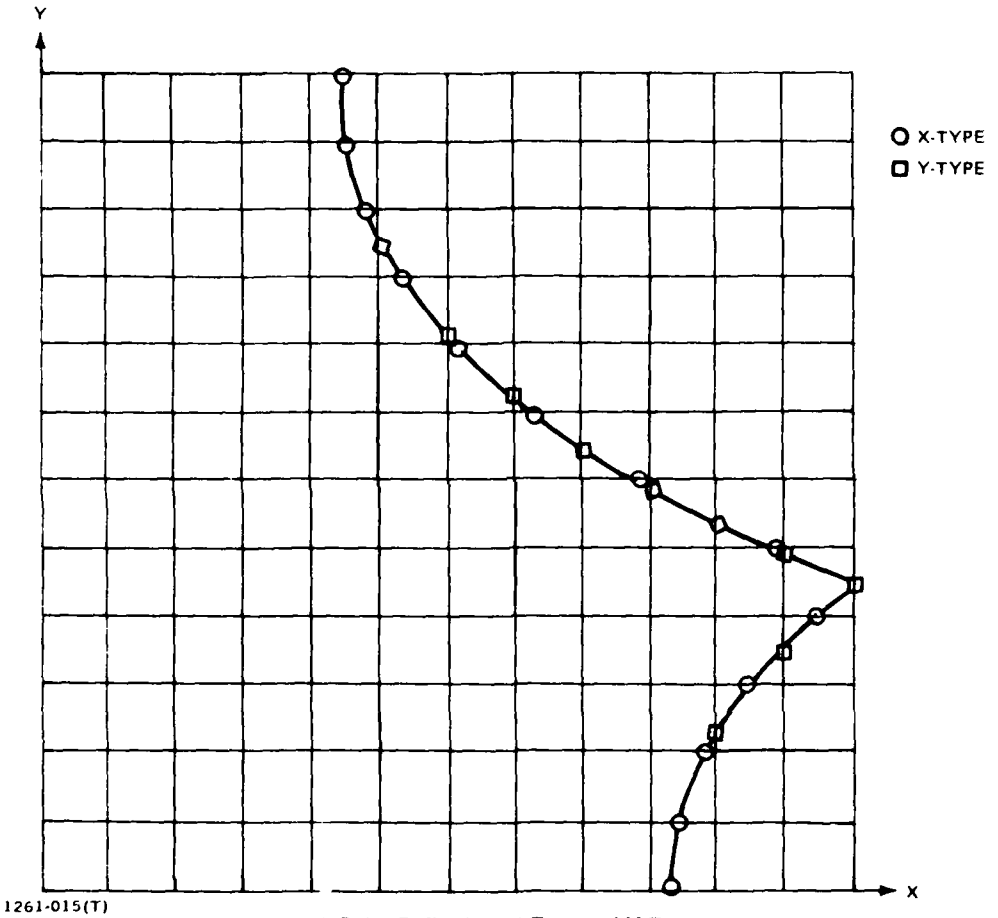

Fig. 15 Shock Point Definition, X-Type and Y-Type

VIII. REGULAR REFLECTION AND MACH DISC SHOCK CONFIGURATIONS

The terms regular reflection and Mach disc are used here to refer to the conditions at the intersection of a shock and a solid boundary either the plate or store. Figure 16 shows the cross sectional views of these two shock configurations. In Fig. 16(a) the flow is deflected toward the plate as it passes through the incident shock, the flow transitions from free stream conditions 1 to conditions 2. In order to satisfy the boundary condition of tangency to the plate the flow behind the incident shock (conditions 2) must pass through a reflected shock to come to the final conditions 3. This phenomenon is two-dimensional only in a plane normal to the intersection of the incident shock and the solid boundary, and this will be discussed in more detail later, the point here is that the free stream conditions used in this local computation are projected into this plane. As the computation proceeds downstream the projected component of Mach numbers decreases; in addition, the projected flow deflection also increases. There will always come a marching station where the deflection needed from condition 2 to condition 3 can't be met with a shock; from this station on the condition at the wall is a Mach disc (Fig. 16b). The point of transition from a regular reflection to a Mach disc seems to be debateable, this issue will be discussed later. The Mach disc configuration has a normal shock at the wall so that the flow tangency condition is met (condition 2, Fig. 16b). The normal shock decreases in strength to a triple point (a confluence of three shocks and a contact). Figures 17(a) and (b) show the regular reflection and Mach disc in the p, θ hodograph plane (i.e., shock polars). The flow angle θ is measured from the free stream velocity direction.

Figure 18 is a three-dimension sketch of an axisymmetric shock impinging of a flat wall. Near the beginning of the interaction the shock reflection is regular. Since the axis of the shock is parallel to the plate the curve formed by the intersection is a hyperbola. At any marching step the two-dimension shock reflection computation is performed in a plane containing the normal to the plate and the normal to the hyperbola. In this plane the flow is locally two dimensional. The conditions behind the incident shock (conditions 2 of Fig. 16(a)) are computed as any other shock point. These

conditions are unaffected by the presence of the plate. Given the conditions in front of the reflected shock it is a simple matter to compute the conditions behind the reflected shock (state 3 of Fig. 16a). The tangency condition is enough to determine the reflected shock.

Once the regular reflection is transitioned to a Mach reflection the conditions at the solid surface are changed. The foot of the Mach stem must be normal to the solid surface in order to satisfy the tangency condition. The velocity on the low pressure side of the shock is tangent to surface (condition 1 of Fig. 16b) therefore the only way to satisfy tangency on the high pressure side is to force the normal to the shock to lie in the surface of the solid boundary. This condition is substituted for the numerical evaluation of the shock's cross slope; the computation then proceeds as discussed in the previous section. There are no special provisions made for the triple point in the case of a Mach reflection. The computation proceeds normally and the triple point naturally develops and floats between mesh points. Logic had to be developed which avoids differencing for the shock slope across the triple points in the flow field. The shock slope at points adjacent to the triple point are taken one sided away from the triple point. Both the regular and Mach reflection computations are identical whether the shock reflects off the store or the plate.

An as yet unresolved problem has been encountered in this work associated with the transition from a regular reflection to a Mach disc. The problem is associated with a difference in pressure and flow direction at the transition point on the solid boundary. For the sake of simplicity let us consider the case of an axisymmetric shock reflecting off a flat plate, an identical phenomenon occurs when the shock reflects from a circular cross section store. The intersection of the shock and the plate is a simply computed hyperbola (Fig. 18). Figure 19 shows the computed pressure and flow angle σ behind the regular reflection in addition to the conditions behind a normal shock traveling along the same hyperbola. In the case plotted the shock was produced by a 15 deg half angle cone at a Mach number of 2.5. The figure shows that at detachment ($z = 2.375$) there is a significant difference in the pressures and flow directions produced by the regular reflection and a normal shock tangent to the hyperbola. In itself, this pressure difference would not be a problem except that in order to match the pressure behind the

regular reflection the normal shock must be reduced in strength. In order for the normal shock to produce a pressure close to that found behind the regular reflection it must move inside the hyperbola (Fig. 20a). The Mach stem must disturb the flow before the location where the axisymmetric shock would have hit the plate (Fig. 20b); unless this flow is disturbed by the Mach stem a regular reflection will exist and this is a contradiction. There is no slope for the base of the Mach stem on the plate which will match both the pressure and flow direction produced by the regular reflection. The possibility of both Prandtl-Meyer expansions and shocks in the plane of the plate has been studied but none of these singularities can transition the regular reflection pressure and flow direction to that of a normal shock moving with a slope higher than that of the hyperbola. The difference in pressure at the detachment point is reduced with increasing the free stream Mach number. In fact, these pressures can be made to essentially match at $M_\infty = 3$ for a cone of half angle 20 deg (this is the case considered in Section IX), and even in this case the flow directions do not match.

The shock capturing results of Fig. 12 were studied in detail to try to understand how this computation handled transition. As is the case in most phenomena of this type the shock capturing results are not detailed enough to identify the problem. The transition phenonenon can turn out to have a significant effect on the flow field, and therefore a significant impact on the forces on the store and/or plate. For example, an additional wave could be developed at transition and ultimately impinge on the store. This is why it is important to understand the physics of the problem even from a practical point of view.

The transition phenomenon has been investigated by a number of previous authors (Ref 18 and 19 for example) and none have been able to formulate a model for the transition from a regular reflection to Mach disc. The standard condition to determine the point of transition (due to von Neumann) imposes that it occurs when the flow deflection required by the reflected shock is equal to the detachment deflection for the local Mach number. This condition is shown in the shock polar of Fig. 21a; surely a regular reflection can not exist beyond this condition. Ben-Dor (Ref 19) proposed that the Mach stem forms slightly sooner, at the point when the projected Mach number behind the reflected shock is sonic (Fig. 21b). This criterion was tried in the present

work with no success. Finally, Henderson et al (Ref 18) proposed a "mechanical equilibrium" criterion for transition. This criterion imposes that the Mach stem forms when the pressure behind the regular reflection matches that behind a tangent normal shock (Fig. 21c). Henderson's condition accounts for the difficulty in resolving the pressure difference at transition but does nothing about the substantial difference in flow direction. Additionally, the Henderson condition can only be applied in the larger Mach number range (in the present problem $M_\infty > 3$) because the von Neumann condition is reached first at lower Mach numbers. Considered, for example, Fig. 19a which shows that the regular reflection pressure and normal shock pressure never match in the case shown. The Henderson condition was tried in the present work with no success. The possibility of more exotic shock configurations have also been considered. The "complex-Mach reflection" and "double-Mach reflection" (Ref 19) has been studied but it seems neither can resolve both the pressure and flow direction differences. There is experimental evidence (Ref 20 and 21) that for the problem considered here the simple Mach disc configuration occurs. The vapor screen photograph of Fig. 22 (supplied by Noel Talcott, NASA/LRC) shows a cross sectional view of the shock configuration for a store/ plate combination at $M_\infty = 6$. The figure shows the standard Mach disc configuration. The future directions of research in the area of shock reflection transition are discussed in Section X of this report.

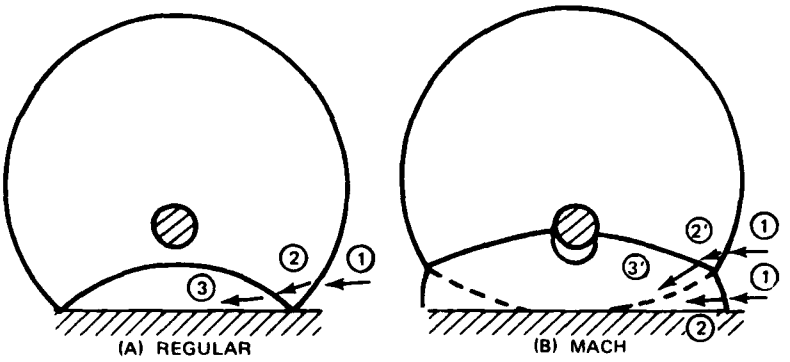

1261-016(T)

Fig. 16 Regular and Mach Reflection Shock Configurations

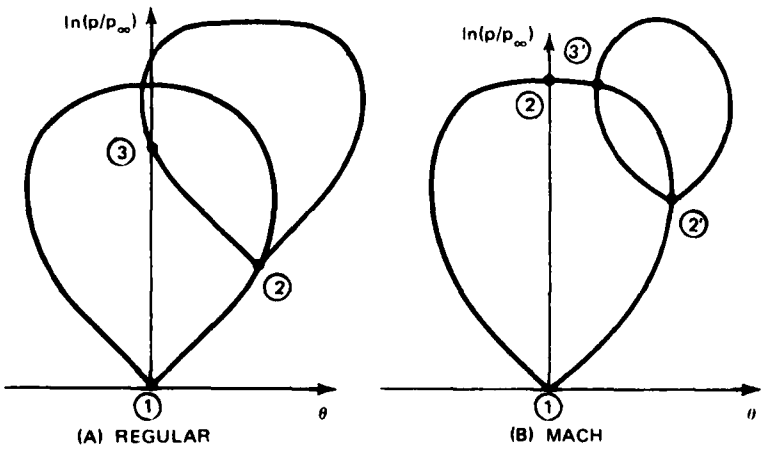

1261-017(T)

Fig. 17 Regular and Mach Reflection, Shock Polar

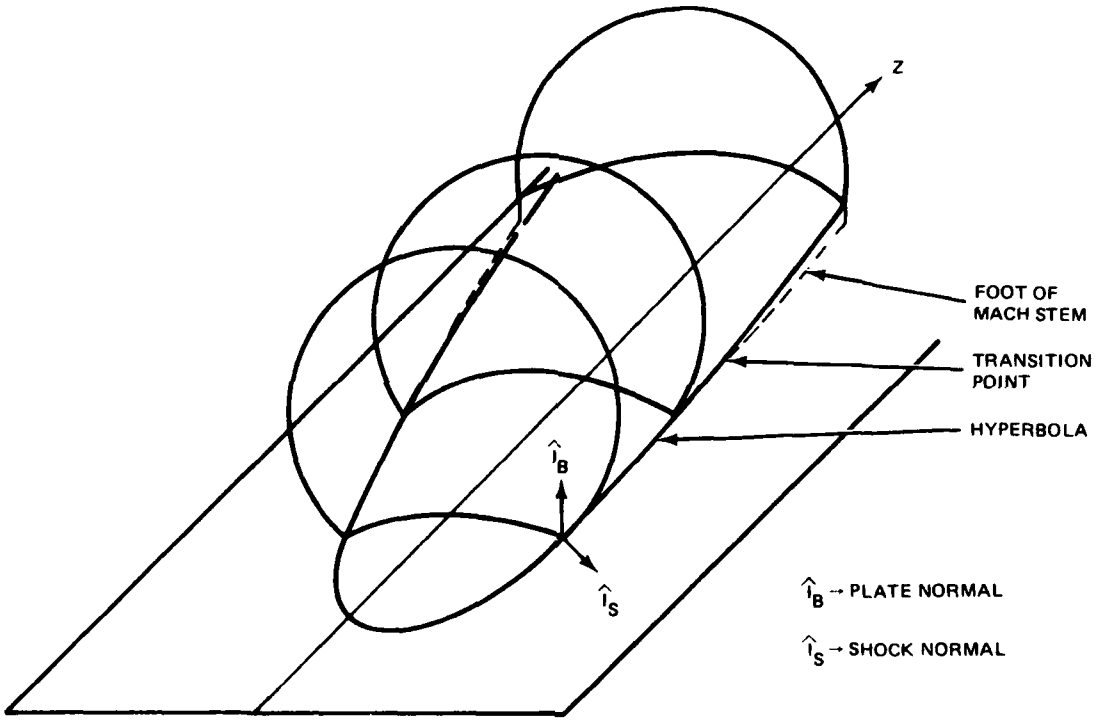

Fig. 18 3-D Sketch of Interaction, Shock/Plate Interaction is 2-D in $\hat{i}_B$ - $\hat{i}_S$ Plane

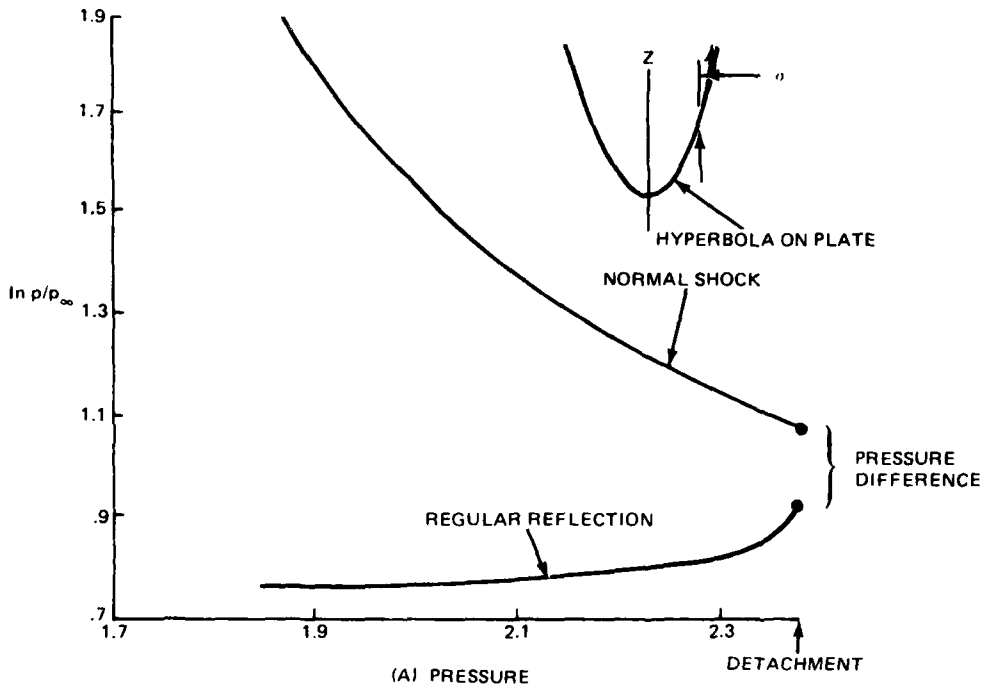

(A) PRESSURE

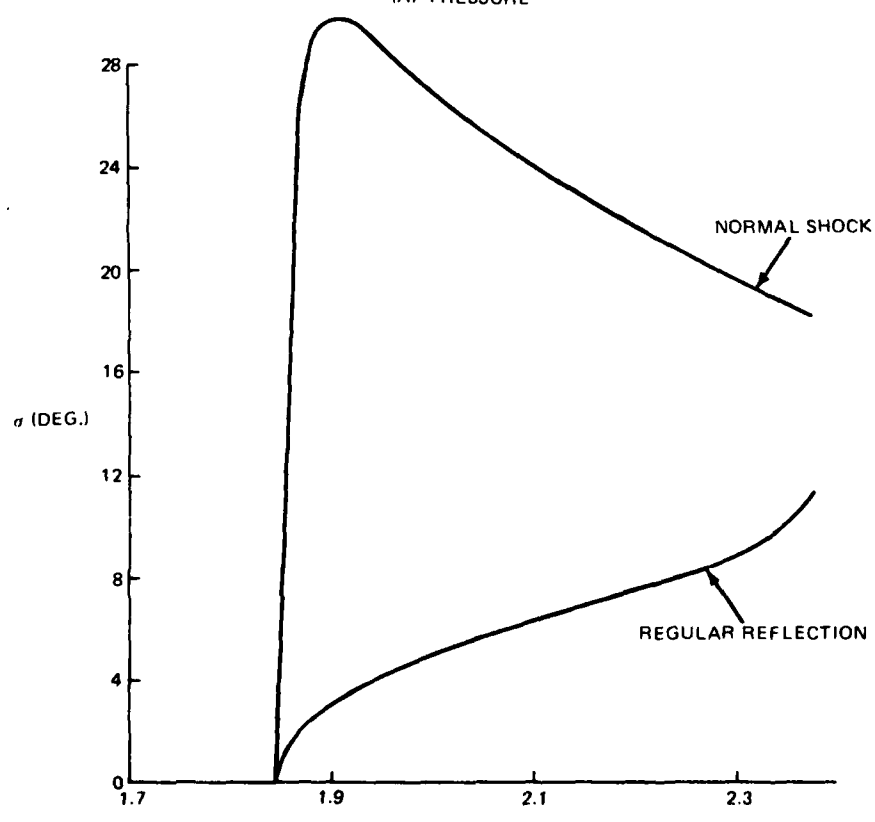

(B) FLOW ANGLE

1261-019(T)

Fig. 19 Flow Field Behing Regular Reflection and Tangent Normal Shock on Plate (M_∞ = 2.5, Cone Half Angle 15°)

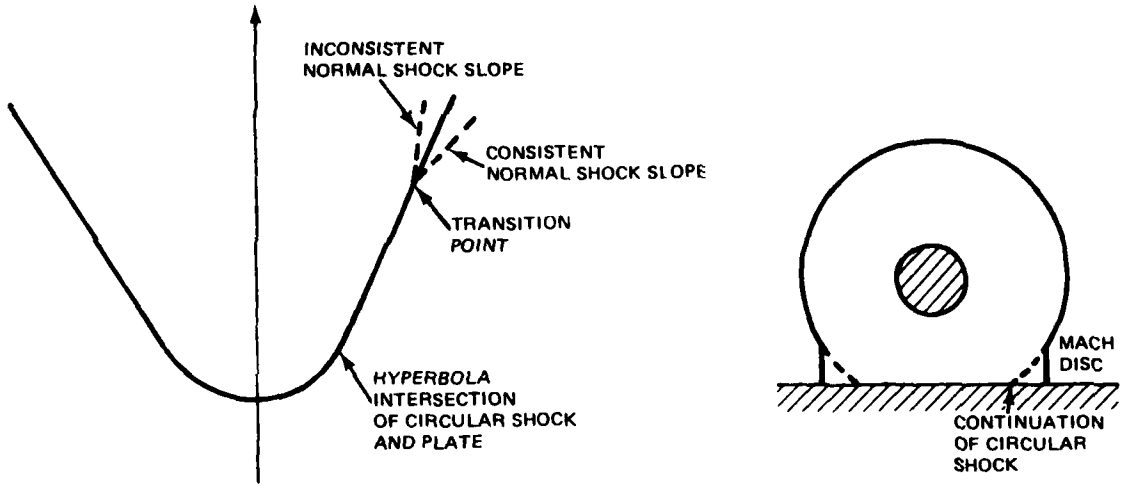

1261-020(T)

Fig. 20 Relative Locations of Mach Disc and Undisturbed Circular Shock

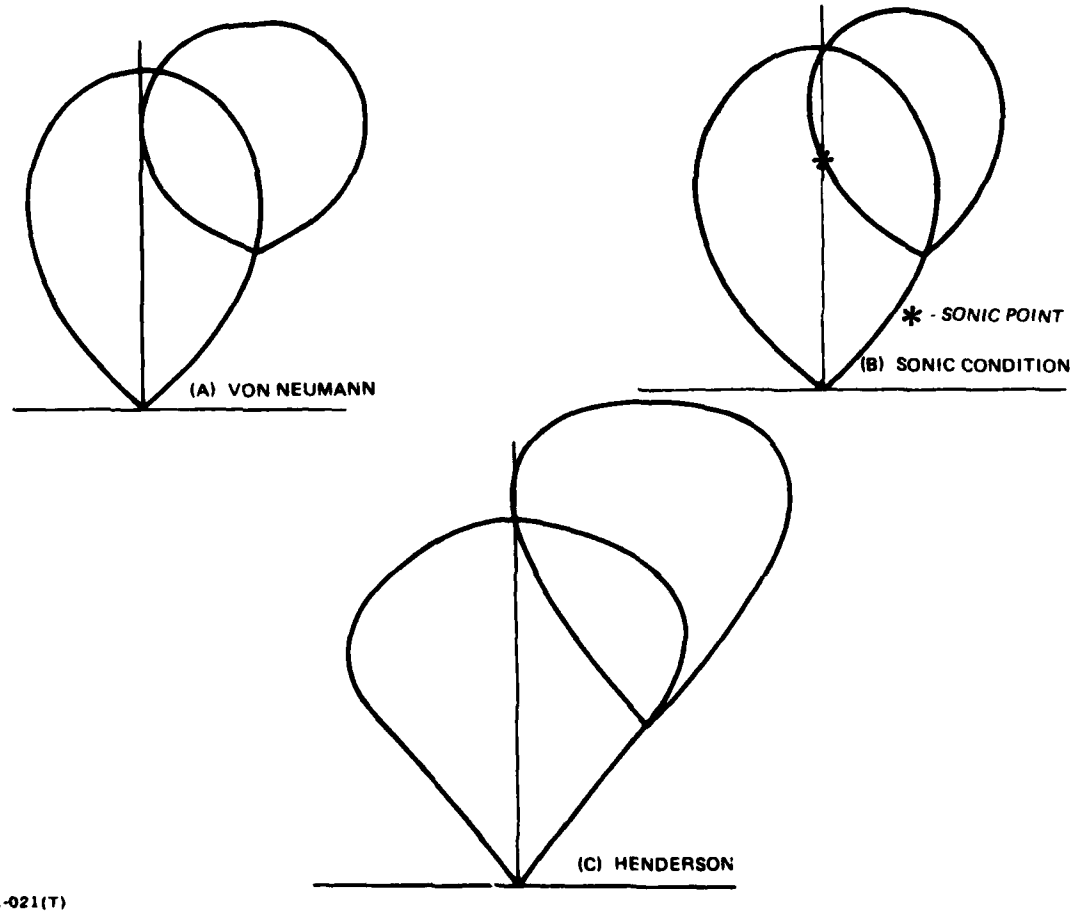

1261-021(T)

Fig. 21 Transition Criterion

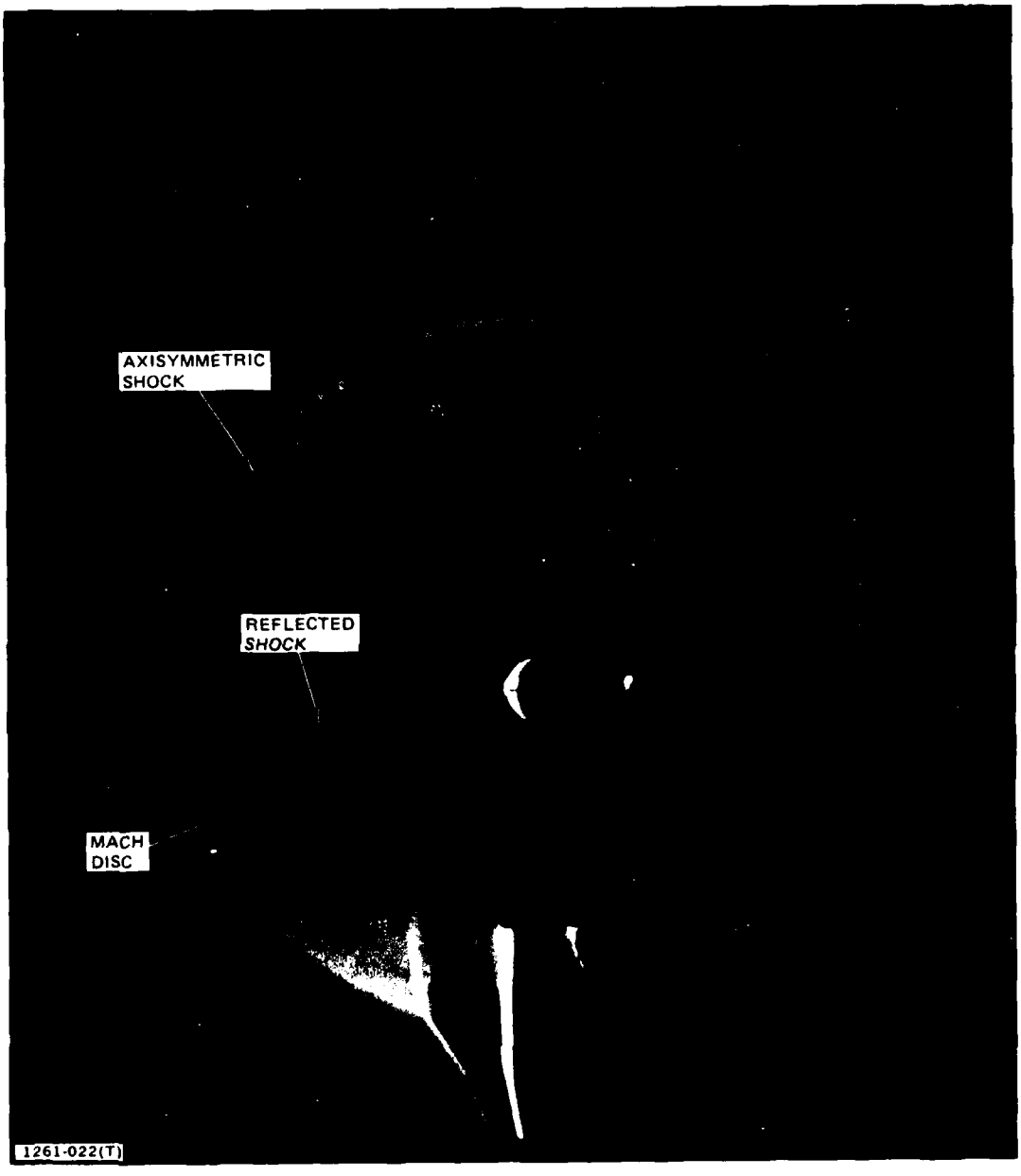

Fig. 22 Vapor Screen Showing Experimental Shock Configuration, Simple Mach Disc

IX. SAMPLE CALCULATIONS

A number of the elements of the computational procedure used in this work were tested early in computing the shock capturing results of Fig. 12. These computations demonstrated the basic finite difference scheme in conjunction with the conformal mapping used. In addition, the results of Fig. 12 showed that the fully three-dimensional flow field (the region below the dashed line of Fig. 12) could be matched with the axisymmetric, undisturbed store flow field. Care had to be taken with this matching in order to avoid computational difficulties at the interface.

The shock between mesh point scheme used to fit the complex shock pattern encountered in this flow field was essentially untested. There has been some previous work in this area (Ref 16 and 17) but none of these came close to developing a scheme which can handle the complex shock patterns encountered in the store separation problem. Therefore, the shock fitting scheme used here had to be tested very carefully at each stage of development. In order to test the basic concept an axisymmetric shock was computed. The grid used was developed by the conformal mapping discussed in Section IV; this grid is not axisymmetric so that the shock crosses grid lines of both families. Figure 23 shows the results of this test computation. The results computed with the three-dimensional shock fitting code are compared with the results of an axisymmetric computation. The comparison is very good, proving that the basic shock fitting scheme is sound.

The real test for the shock between mesh point scheme came in computing shock reflections. Figure 24 shows a computed shock configuration for a store/plate combination at $M_\infty = 3$ and a cone half angle of 20 degs. This computation is impressive because it shows how the shock between mesh point scheme can handle all the geometric complexities of the shock pattern produced by a store plate interaction. The problem of transition from a regular reflection to a Mach disc was handled in this computation in an ad hoc fashion. For these conditions the pressure behind the regular reflection at detachment is equal to that behind a tangent normal shock. The foot of the Mach stem was computed by keeping this pressure constant. The results of Fig. 24 show that the shock between mesh point scheme can handle triple points near

the plate and store simultaneously ($z \approx 3.1$, at the store there is a small Mach stem). This computation indicated that except for the problem of transition, the code which is under development can predict complex interactive flow fields.

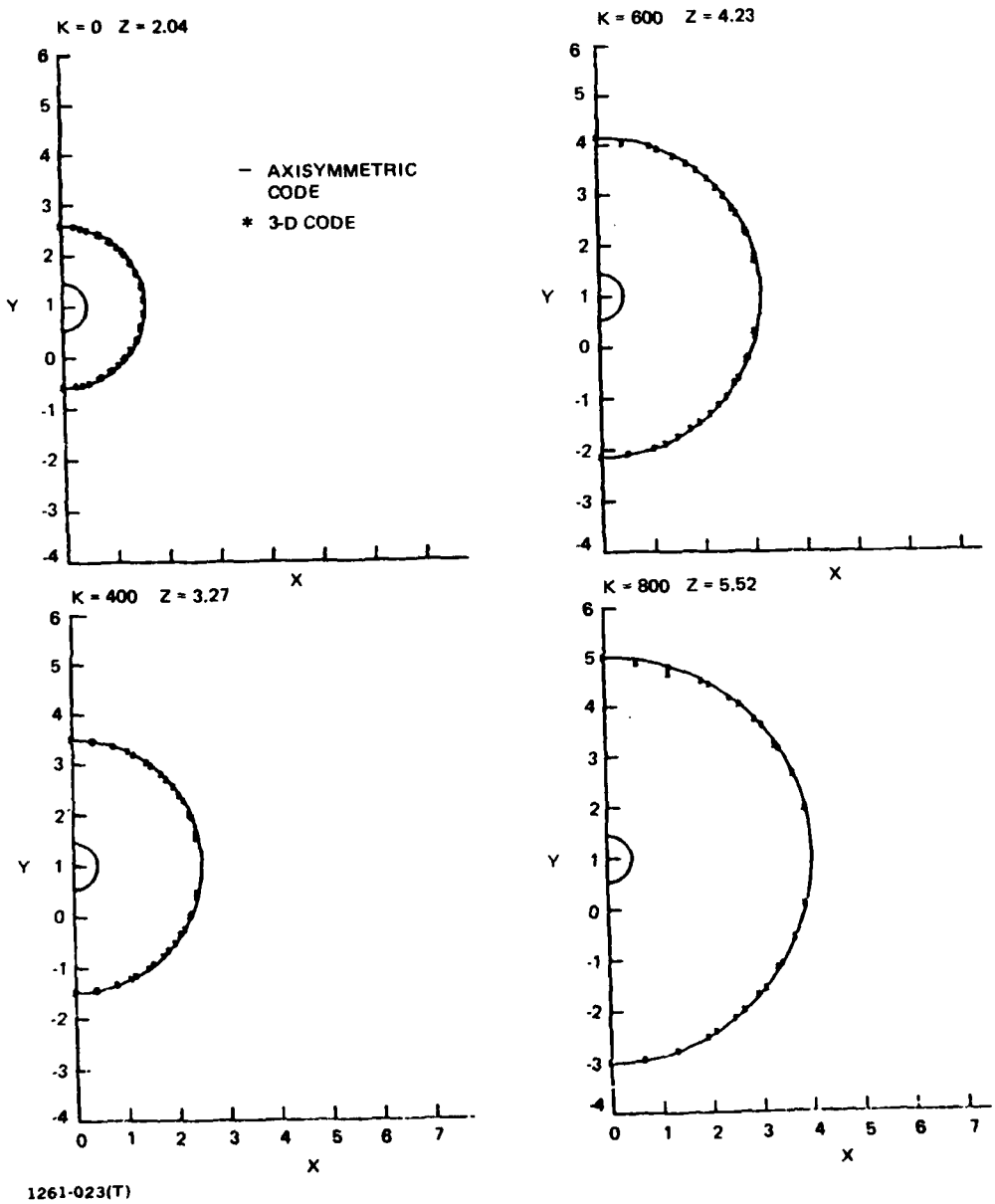

Fig. 23 Shock Shape Comparison

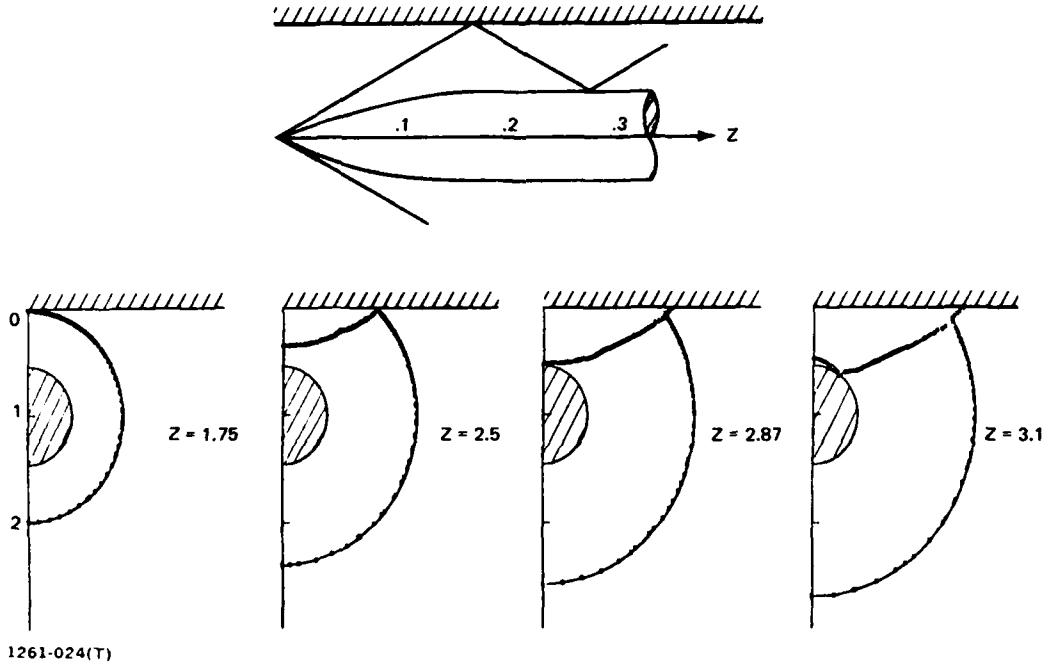

Fig. 24 Computed 3-D Shock Shapes, Fitted Shock Between Mesh Points ($M_\infty = 3$, Cone Half Angle = 20°)

X. CONCLUSIONS AND FUTURE DIRECTIONS

The goal set forth at the outset of this work was to develop a code which can be used to predict the interactive flow field of store separation. In the initial phase of this work significant progress has been made toward this end. The sensitivity of the forces on the store to the shock reflection phenomenon has been quantified leading to the conclusion that solutions to Euler's equations are needed to obtain reliable results. A number of shock capturing schemes have been tested and it was found that none of these can be used reliably in the supersonic store separation problem. A simple conformal mapping has been used to generate a good computational grid. The concept of computing only the flow field disturbed by the reflected shock has been combined with a characteristic based finite difference scheme to form the basis of an accurate and efficient computational procedure. From a numerical point of view the most important progress has been made in the area of shock fitting. A very powerful floating discontinuity procedure has been developed. It has been tested and found reliable and its generality has been demonstrated by predicting very complex reflecting shock patterns.

The one question left unanswered is how the shock configuration transitions from a regular reflection to a Mach disc. In order to study this phenomenon carefully a pilot code must be developed. The three dimensional code now being used for these computations is complicated by the new shock between mesh point scheme. The pilot code would be much simpler and directed toward studying the transition problem. This code would be very similar to the one developed by the author to study the complex shock patterns in conical corner flow fields (Ref 15). In addition to the pilot code an analytical effort will be undertaken to try to develop a transition criterion and a wave pattern which can account for the difference in pressure and velocity slope between the regular reflection and simple Mach reflection. It would seem that (at least in part) the difference in velocity slope can be accounted for by the contact surface which develops in conjunction with the Mach disc. This possibility will be studied with the simple pilot code.

In addition to the transition problem there are a few minor problems with the code which has been under development during this one year effort.

This code now serves as a numerical research tool; it must be streamlined in order to study the store separation process. The scheme used to compute the shock cross slope seems to cause minor wiggles in the shock, this is apparently a coding problem which can be eliminated with a small effort. Once the transition problem is understood the streamlines code will become available for the detailed study of interactive flow fields. The code must then be modified in order to be able to compute store/plate flow fields when the store is at an angle of attack relative to the plate. With this capability a series of computations describing the separation process can be made. The position and orientation of the store relative to the plate can be predicted based on the forces and moments computed on the store at any instant during the separation process (the unsteady fluid mechanics being negligible). In this manner the entire separation process can be predicted.

XI. REFERENCES

1. Gapcynski, J. P. and Carlson, H. W., "A Pressure-Distribution Investigation of the Aerodynamic Characteristics of a Body of Revolution in the Vicinity of a Reflection Plane at Mach Numbers of 1.41 and 2.01," NACA RM-L54J29.

2. Moretti, G., "The λ-Scheme," J. Comp. and Fluids, 7, 191, 1979.

3. Marconi, F., Salas, M., "Computation of 3-D Flows About Aircraft Configuration," J. Comp. and Fluids, 1, 185, 1973.

4. Marconi, F., Salas, M. and Yaeger L., "Development of a Computer Code for Calculating the Steady Super/Hypersonic Inviscid Flow Around Real Configurations," NASA CR 2675, 1975.

5. Salas, M. D., "Shock Fitting Method for Complicated Two-Dimensional Supersonic Flows," AIAA J., Vol. 14, No. 5, 1976.

6. Kutler, P., Lomax, H. and Warming, R. F., "Computation of Space Shuttle Flow Fields Using Noncentered Finite Difference Scheme AIAA Paper No. 74-193, 1972.

7. Steger, J. and Warming, R., "Flux Vector Splitting of the Inviscid Gas Dynamic Equations With Application to Finite Difference Methods," NASA TM 78605, 1979.

8. Grossman, B., "Numerical Procedure for the Computation of Irrotational Conical Flow," AIAA J., Vol. 17, No. 8, August 1979.

9. Jameson, A., "Iterative Solution of Transonic Flow Over Airfoils and Wings, Including Flows at Mach 1," Comm. Pure Appl. Math., Vol. 27, May 1974, pp. 283-309.

10. Mac Cormack, R. W., "The Effects of Viscosity in Hypervelocity Impact Cratering," AIAA paper no. 69-354, 1969.

11. Abbett, M. J., "Boundary Condition Computational Procedures for Inviscid Supersonic Steady Flow Field Calculations," Aerotherm Corp., Mt. View, California, Final Report, 71-41, 1971.

12. Rudman, S., "Multinozzle Plume Flow Fields," AIAA Paper 77-710, 1977.

13. de Neef, T. and Moretti, G., "Shock Fitting for Everybody," to appear in J. Comp. and Fluids.

14. Moretti, G., Grossman, B., and Marconi, F., "A Complete Numerical Technique for the Calculation of 3-D Inviscid Supersonic Flow," AIAA Paper No. 72-192, 1972.

15. Marconi, F., "Internal Corner Flow Fields," AIAA J. Vol. 18, No. 1, 1980.

16. Moretti, G., "Three-Dimensional Supersonic Steady Flow with Any Number of Imbedded Shocks," AIAA Paper No. 74-10, 1974.

17. Rudman, S., "Multinozzle Plume Flow Fields," Grumman Research Report, RE-618, 1980.

18. Henderson, L. F. and Lozzi, A., "Experiments on Transition of Mach Reflection," J. Fluid Mech., Vol 68, Pt. 1, pp. 139-155, March 1975.

19. Ben-Dor, G., "Regions and Transitions of Non-stationary Oblique Shock-Wave Diffractions in Perfect and Imperfect Gases", UTIAS Report No. 232, August 1978.

20. Bryson, A. E. and Gross, R. W., "Diffraction of Strong Shocks by Cones, Cylinders and Spheres," J. Fluid Mech., Vol. 10, 1960.

21. Talcott, N. A., Private Communication.


DATE
ILME
8